To The Graduate Council:

I am submitting herewith a dissertation written by Melissa McManis Armstrong entitled "Design, Development, and Evaluation of Fiber-Optic Chemical Sensors for Fluoroimmunoassays." I have examined the final copy of this dissertation for form and content and recommend that it be accepted in partial fulfillment of the requirements for the degree of Ph.D., with a major in Chemistry.

M J Sepaniak

Michael J. Sepaniak, Major Professor

We have read this dissertation and recommend its acceptance:

Geo. K. Schweitzer

Carl P. Enke

Thurbide

Accepted for the Council:

Associate Vice Chancellor
and Dean of The Graduate School

Design, Development, and Evaluation of Fiber-Optic Chemical Sensors for Fluoroimmunoassays

A Dissertation
Presented for the
Ph.D
Degree
The University of Tennessee, Knoxville

Melissa McManis Armstrong
December 1994

DEDICATION

This dissertation is dedicated to my parents

Kenneth and Charlotte McManis

and to my husband

Jeff Armstrong

"Your love has given me great joy and encouragement"

Philemon 7

Thanks, I love you. I couldn't have done it without you.

Acknowledgements

I would like to acknowledge the support of my major professor, Dr. Michael Sepaniak and the members of my committee, Drs. George Schweitzer, E. L. Wehry, and Paul Bienkowski.

This research was funded by the National Institutes of Health, the National Science Foundation, and the Department of Energy.

I'd also like to acknowledge the support of Mr and Mrs S. Robert Armstrong, who provided me with food and lodging when I travelled to Knoxville to work on this dissertation.

ABSTRACT

Immunoassays are the method of choice for detection and monitoring of many biological markers. This research combines the specificity and sensitivity of fluoroimmunoassay techniques with several fiber-optic chemical sensor protocols. The goal was to design a sensor that could be used for continuous or repetitive *in situ* analysis of large molecules such as proteins. Immunoglobulin G (IgG) is used as a representative protein molecule.

Several prototype sensors are described. These sensors revealed that immobilization of antibody-containing silica spheres (immunobeads) near the end of an optical fiber gave the largest concentration of antibody in the sensing range of the fiber. Immobilization of the immunobeads was accomplished by entrapment behind a membrane or frit. Protein molecules are too large to be sampled by diffusion, so a method for sampling by aspiration was developed. Reagent delivery into the sensing chamber by way of capillary columns made delivery of reagents in multi-step immunoassays more practical and allowed the sensors to be regenerated between trials. The early sensors revealed the importance of reproducibility of antibody coverage on the immunobeads. Other factors that were studied with these sensors were the density and volume of the bead slurry and the flow rate for reagent and sample delivery.

A sensor molded from acrylic resin was designed. This sensor was similar to the capillary column sensor, but the resin was more resistant to aqueous solvents than the epoxy used in the earlier sensors. It was found that the optimum immunobead conditions for this sensor were 50 μl of a slurry with density of 10 mg silica/ml. Optimum flow rate for this sensor was 136 μl/min. A direct immunoassay for fluorescently-labeled IgG was used to illustrate the function of the sensor and to aid in development of a sandwich immunoassay for the sensor. A calibration curve for the direct assay is exhibited. This sensor gave a limit of detection of less than 0.005 mg/ml of IgG using the direct assay protocol.

There are many more variables in a sandwich assay than in a direct assay. The slurry concentration, flow rates of sample, rinse and second antibody solutions, and the concentration of the antibody solution must all be controlled. Careful selection of the antibody system is crucial for a successful sandwich immunoassay. The epitope of the analyte molecule bound by the immobilized antibody must be well separated from the epitope bound by the free antibody to allow room for binding of both antibodies to the analyte. This may be best accomplished with the use of monoclonal antibodies developed to greatly separated portions of the analyte molecule. Analyte molecules with two distinct portions, such as leutinizing hormone with α and β subunits, may be more amenable than IgG to analysis by sandwich immunoassay using the sensors developed in this work.

TABLE OF CONTENTS

LIST OF TABLES

LIST OF FIGURES

LIST OF ABBREVIATIONS

Abbreviation	Represents
Ab1	Anti-rabbit IgG, usually the immobilized antibody
ATP	Adenosine triphosphate, part of the biochemical energy transfer cycle
CDI	1,1 carbonyl diimidazole
CV	coefficient of variation
F(ab)	Antigen binding fragment of immunoglobulin
F(c)	Constant portion of immunoglobulin
FIA	Fluorescence immunoassay
FITC	Fluorescein isothiocyanate
FITC-IgG	FITC-labeled IgG molecule
FOCS	Fiber Optic Chemical Sensor
GOPS	glycidoxypropyltrimethoxysilane
hCG	Human choriogonadotropin, produced by the placenta during pregnancy and by certain cancers
IgG	Immunoglobulin G, an antibody protein molecule
MW	Molecular Weight
MWCO	molecular weight cutoff, refers to membranes
NA	Numerical Aperature

NAD^+	Nicotinamide adenine dinucleotide, a biological carrier of electrons, accepts 2 electrons and a proton from a substrate undergoing metabolic oxidation
NADH	Reduced nicotinamide adenine dinucleotide
PBS	phosphate buffered saline solution, generally buffered to pH 7.0-7.6
PCS	Plastic Clad Silica Optical Fiber
RITC	Rhodamine B isothiocyanate
TRITC	Tetramethyl Rhodamine B isothiocyanate
TRITC-Ab2	TRITC-labeled anti-rabbit IgG, the second antibody in a sandwich assay
TRITC-IgG	TRITC-labeled immunoglobulin G

CHAPTER 1

BASIC PRINCIPLES OF FIBER OPTIC CHEMICAL SENSORS

The development of real-time sensors for a variety of chemical and biochemical analytes has been the goal of a large volume of research during the last 15 years. Sensors are devices capable of continuous and reversible measurement of analyte concentration. Ideally such sensors should allow direct in situ analysis without the need for conventional sampling, addition of reagent, or dilution(1).

Real time analysis/continuous monitoring is desirable in a number of settings. The ability to operate such sensors remotely or using robotics expands their applicability to hostile or inaccessible environments. Hazardous material processing/storage facilities, process control in manufacturing, and therapeutic drug monitoring are only a few of the potential applications.

A variety of transducers have been developed which are sensitive to changes in optical, thermal, electrochemical and mass properties in the sensing region. Electrochemical methods are among the most developed, using potentiometry and voltammetry to monitor a variety of analytes ranging from H^+ to neurotransmitters (2, 3). Optical sensor technology has expanded rapidly with the coupling of conventional spectroscopic techniques with fiber optics.

Recent advances resulting in rugged, small diameter optical fibers with low attenuation, lower cost lasers and light emitting diodes with output ranges from 450-1000 nm, and less expensive but sensitive photodetectors and amplifiers, have contributed greatly to advances in optical sensing.

Principles of Fiber Optics

Parts of an Optical Fiber

Figure 1.1 illustrates the basic elements of a fiber optic. The fiber consists of a cylindrical core surrounded by a cladding. A protective jacket usually surrounds the cladding. The core and cladding are usually made of plastic, glass, or quartz and have different refractive indices.

Light Transmission Properties

A basic understanding of the transmission of light through different media is necessary to understand the principles of fiber optics.

When a light ray is incident on a transparent material some portion of the light is reflected with the angle of reflection equal to the angle of incidence. Light which is not reflected is refracted into the material at an angle different from the angle of incidence. Snell's Law (Equation 1) relates the angles of incidence and

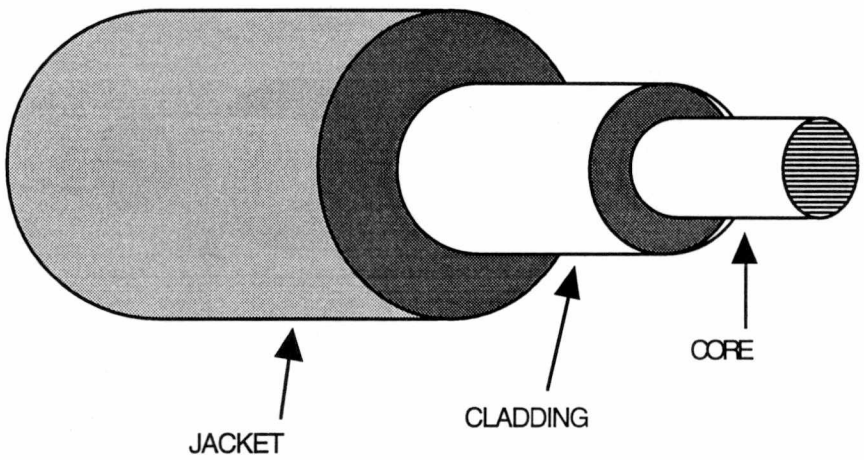

Figure 1.1. Cross-sectional view of an optical fiber.

refraction to the refractive indices of the media.

$$\eta_1 \sin\theta_1 = \eta_2 \sin\theta_2 \qquad (1)$$

where η_1 and η_2 are the refractive indices of the media and θ_1 and θ_2 are the angles of incidence and refraction respectively.

When glass is in contact with a material of lower refractive index, light is refracted only up to a maximum angle of incidence. Beyond this angle of incidence, the light is reflected back into the glass; a situation called total internal reflection. Snell's law allows us to define a relationship between this critical angle and the refractive indices. For total internal reflection to occur θ_2 must be at least 90°. This occurs when $\sin\theta_1 \geq \eta_1/\eta_2$.

This principle of total internal reflection is the basis of light transmission in optical fibers. Total internal reflection depends on the refractive index of the surrounding medium and the indices of the core and cladding. Varying the refractive indices of the core and cladding allow the construction of fiber optics with a variety of light collection and transmission properties. Step-index fibers employ a core material with a constant refractive index and a cladding with a smaller refractive index. Gradient index fibers use a core with a refractive index that decreases parabolically from the center of the core toward the cladding.

Figure 1.2 is an illustration of the geometrical optics model of light propagation in a multi-mode step-index fiber. Using this model

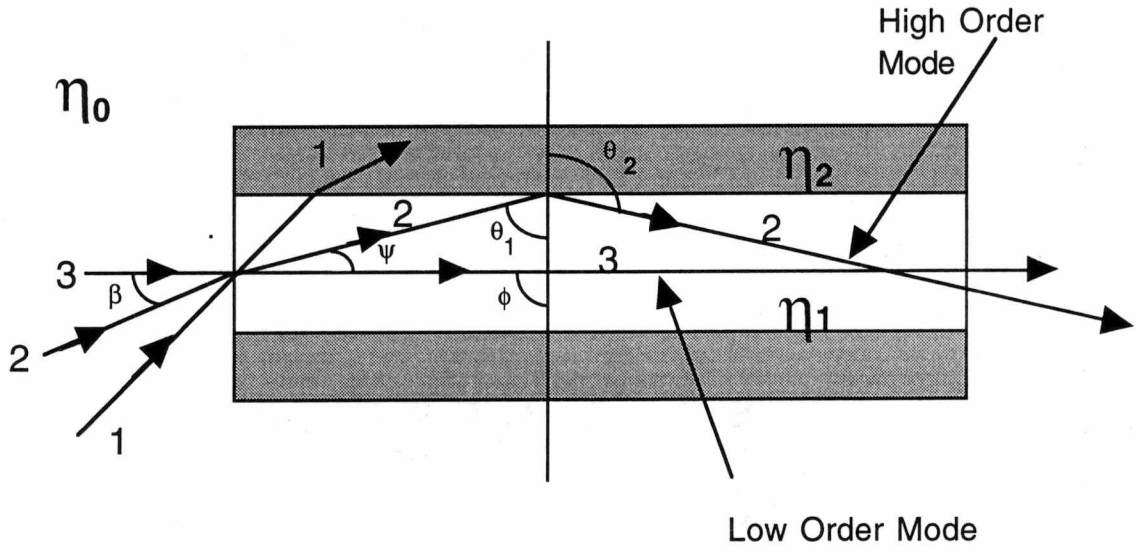

Figure 1.2. Geometrical optics model of light propagation in a multi-mode step-index fiber.

and Snell's law, equation 2 can be derived to describe the maximum half acceptance angle (β) of light entering the fiber:

$$\sin\beta = \frac{(\eta_1^2 - \eta_2^2)^{\frac{1}{2}}}{\eta_0} \qquad (2)$$

where η_0 is the refractive index of the material surrounding the fiber, and η_1 and η_2 are the refractive indices of the core and cladding respectively. Two other parameters are frequently used to describe fiber optics. They are numerical aperture, NA, and f/number, and are defined by equations 3 and 4, respectively.

$$NA = \eta_0 \sin\beta \qquad (3)$$

$$f/_{number} = 1/_{(2\tan\beta)} \qquad (4)$$

This model does not take into account interference effects. A very rigorous description of the optics involved in fiber-optics sensors, including solutions of Maxwell's equations has recently been published (4). These solutions lead to the conclusion that light propagates in discrete modes through the fiber. Each mode corresponds to a different incidence angle. The number of modes that a fiber can carry depends on the diameter and numerical aperture of the fiber; this relationship is described by equation 5 (1).

$$N_m = 0.5\left(\frac{\pi \cdot d \cdot NA}{\lambda}\right)^2 \qquad (5)$$

Gradient index, single mode fibers have diameters so small (3-5 μm) that only a single mode of light is transmitted. This type of fiber has the capability to maintain the temporal and phase relationships of the light coupled to the fiber optic and is generally used in telecommunications applications or for interferometer based sensors. The low light throughput does not make them very amenable to use in the majority of fiber optic sensor applications. Fibers with larger numerical aperatures (more modes) have a higher light collection efficiency and greater throughput, since there is more than one pathway through the fiber. This makes them more amenable to use in the extrinsic sensors described in the next section.

When total internal reflection occurs at the interface between two materials, the light is not instantaneously reflected but rather travels some distance into the lower refractive index material (Figure 1.3). The light penetrating the outer material is called the evanescent wave. This evanescent wave property is exploited in a number of intrinsic sensors discussed in a later section.

The wavelength of light transmitted by an optical fiber is dependent upon the core material. Most optical fibers are SiO_2 glasses. The transmission wavelength for the silica core is from approximately 300 to 1700 nm. Zirconium fluoride glasses extend the transmission wavelength well into the IR. Plastic fibers have a range that is limited to 400-800 nm.

Two types of step-index, multi-mode, optical fiber have been used in this research. Most of the early research was performed

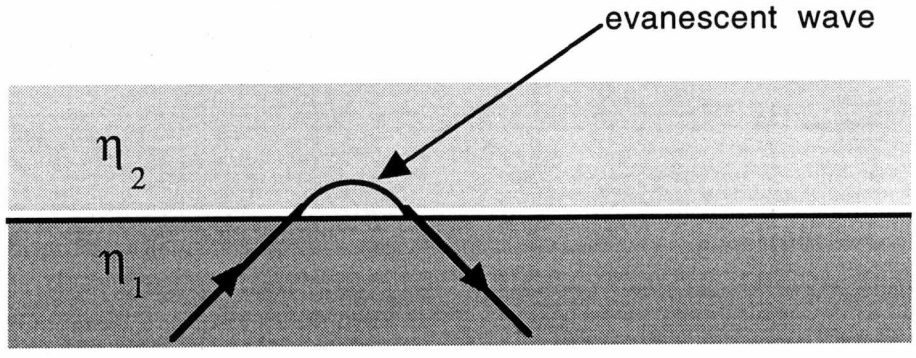

Figure 1.3. Evanescent wave at the interface of optical media where $\eta_2 \leq \eta_1$.

using soft plastic clad silica (PCS) (η_1=1.47, η_2=1.40). Later research employed hard PCS (η_1=1.47, η_2=1.42). Hard PCS offered the advantage of a core and cladding that are more integrally bonded. This meant that the fiber core was less likely to "piston" out, a property which turned out to be very important in sensor applications. This advantage was gained at a slight cost, since the hard PCS had a smaller numerical aperature relative to the soft PCS, slightly reducing its light collecting ability.

Principles of Fiber Optic Chemical Sensors

Sensor Configurations

Fiber optic chemical sensors (FOCS) generally fall into two broad categories. Plain-fiber or direct sensors measure a spectral property of the analyte such as absorbance or fluorescence. Indirect sensors require interaction of the analyte with a reagent phase immobilized on or near the sensing terminus to produce an optically measurable property. Each sensor type can be further subclassified as either an intrinsic or extrinsic sensor. Intrinsic sensors respond to changes in the light transmitting characteristics of the fiber. In extrinsic sensors the fiber is merely a "light pipe" leading to and from the sample and it is the spectral properties of the sample that are probed.

Direct Sensors

Plain-fiber methods offer the advantages of ruggedness and simplicity. They usually are stable over long time periods, making them amenable for use in hostile environments where frequent changing of sensors is undesirable or impossible. Calibration and operation are simple and frequently easily automated. As a whole, plain fiber sensors are less selective and sensitive than indirect sensors and are limited to a relatively small number of analyte molecules with absorbances and emissions in the UV/VIS/NIR regions transmitted by optical fibers. These sensors have found greatest applicability in industrial and environmental monitoring, particularly in situations where fairly large changes in concentration are measured, or where good selectivity is not necessary.

Intrinsic sensors. Direct intrinsic sensors generally require modification of a commercial optical fiber or manufacture of a specialized fiber. Commercial fibers designed for telecommunications are usually designed to be resistant to interferences caused by chemical species in the environment. Several intrinsic sensors use glass rod waveguides rather than optical fiber (5). Also common are configurations in which the cladding is stripped from the fiber. Bending the fiber or waveguide allows for deeper penetration of the evanescent wave into the cladding or sample, a property that is frequently exploited in

intrinsic sensors. Intrinsic sensors have the potential for application in areas where response along the whole length of the fiber, rather than only at the end, is desirable. Intrinsic sensors are used to measure refractive index changes and evanescently excited absorbance and fluorescence (5-9).

Extrinsic sensors. Direct extrinsic sensors have been used to measure the native absorbance and fluorescence in samples. Industrial/environmental applications include monitoring the concentration of Cu^{2+} in electroplating baths (10), monitoring CH_4 in natural gas lines (11), detecting UF_6 in flowing streams (12), monitoring phenols and other pollutants in groundwater (13) and solvent mixture analysis (14). Biomedical applications include measuring bilirubin absorbance and adriamycin fluorescence in biological fluids (15,16), monitoring the absorbance changes of colored body fluids, and measuring NADH fluorescence in several different environments (17). Plain-fibers have also been used in detectors for a number of more traditional analytical techniques such as atomic emission spectrometry, liquid chromatography and gas chromatography (17).

Indirect Sensors

The vast majority of FOCS applications found in literature are for indirect FOCS. These sensors expand the applicability of fiber-optics techniques to species without useful absorbance or

fluorescence in the transmission range of optical fibers. These sensors offer greater selectivity and sensitivity as well as broader applicability, and will be the focus of the remainder of this chapter. These sensors will be classified by immobilization method rather than device type.

A variety of methods have been used for immobilization of the reagent phase. These include direct covalent attachment to the fiber, covalent attachment to a membrane, entrapment in a gel, or entrapment in a chamber with an analyte permeable membrane. Figure 1.4 shows some of the immobilization methods.

Direct covalent or noncovalent attachment of reagent to the fiber has been used for enzyme based sensors and antibody based sensors (6, 18-23), but is limited by the amount of reagent that can be bound to the face of the fiber.

A more common arrangement involves attachment of reagents to an optically transparent membrane that is attached to the fiber. This seems to offer the advantage of quick replacement of the reagent phase and the membrane material may be chosen and modified to better suit the particular reagent system. This system has been used in pH analysis, enzyme analyses and immunoassays (24-28). Limitations to these covalent attachment methods are similar; the amount of reagent bound is usually quite small due to low surface area (both the membrane and the fiber are essentially flat), the covalent attachment procedure may denature enzymes and proteins or hinder access to active sites, and the fiber can "see"

a. Direct attachment of reagent to bare fiber

b. Reagent bound to transparent membrane

c. Reagent trapped in polymer or gel

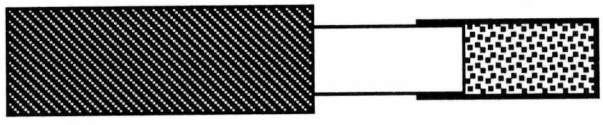

d. Reagent-in solution or on beads-trapped in hollow-fiber membrane or capillary tubing

Figure 1.4. Reagent immobilization methods for FOCS.

well beyond the reagent phase making these procedures more susceptible to measurement interferences.

If the reagents are held in a gel or polymer, covalent attachment is unnecessary, lessening the spatial and denaturing problems associated with covalent attachment. If the gel is thick enough, "see through" effects are diminished. Increasing the thickness of the gel brings longer diffusion times for contact of analyte with reagent, limiting applications to relatively small molecules. This type of sensor has shown some irreproducibility due to swelling of the membranes (29-37).

Entrapment of the reagents within a hollow membrane or tube terminated with a membrane is the most common method of immobilizing reagents for FOCS. If the analyte is much smaller than the reagent, a molecular weight cut-off membrane that allows passage of analyte may be used. This method has been used with diffusion sampling for small analyte molecules (24, 38-44). In the case of analytes and reagents of similar size, or if it is desirable to reject large interferents, it is possible to immobilize the reagent on beads so that it is held in the chamber (45, 46). This poses many of the same risks and limitations associated with direct attachment methods, but has less of the surface area limitation. The use of this technique with large analytes has been limited due to slow diffusion of large molecules through the membrane.

Sensor Chemistry

Sensors such as the indirect sensors described above have been used for a variety of applications. The reagent phase-analyte chemistries employed vary with the intended application and the type of analyte.

Analysis of Small Molecules

Most of the sensors described in literature are for small analyte molecules (MW < 1000 Daltons). pH sensors generally use a dye whose absorbance or fluorescence intensity changes with pH. The most commonly used absorbance indicators are phenol red, chlorophenol red, bromothymol blue, and alizarin. Coumarin and fluorescein derivatives are commonly used for fluorescence pH detection (25, 37, 46-50). Metal ions can be detected by immobilizing a chelating agent that forms a colored complex with the ion (13, 42, 51-56). Fluorophore quenching has been use to detect oxygen, SO_2, some amines, halides, and a number of biologically important molecules including vitamin B and nucleotides (32, 57-60).

Protein Analysis

Larger biomolecules such as proteins and enzymes are more difficult to detect using FOCS. Traditional protein analysis methods that employ spectrophotometric measurements are not all applicable to FOCS. The simplest technique for such analyses is measurement

of the absorbance of protein solutions at 280 nm. This rapid, nondestructive technique is frequently used to screen for overall protein content. The method depends on the absorbance of tyrosine, tryptophan, and phenylalanine residues, resulting in different extinction coefficients for different proteins. Some proteins do not contain these amino acids and thus can not be determined. The method is nonselective and is subject to interferences from nucleic acids, it has a sensitivity range of 0.2 mg/ml to 2 mg/ml (61).

The other commonly used spectrophotometric methods (Bradford assay, Lowry assay, and Bicinchoninic assay) are all destructive of the proteins, but are generally more sensitive, allowing detection of as little as 10 μg/ml. These methods utilize dyes and color development techniques which respond to all proteins in the sample, making the techniques nonselective. These techniques are also subject to a wide range of interferences (61).

Spectroscopic techniques are frequently used in conjunction with a variety of separation techniques used for protein purification. Affinity chromatography uses immobilized antibodies that are specific to the particular protein(s) being determined. Immunoprecipitation allows the selective precipitation of proteins by reaction with specific antibodies, but usually results in denaturation of the protein molecule. Gel electrophoresis has become one of the most widely used separation techniques for protein analysis. Proteins are separated based on their size and charge properties and molecules that differ by a single charge unit

can be separated. The conditions under which gel electrophoresis is performed determine whether the proteins will be denatured. Proteins are then detected by Coomassie blue staining (61). The traditional bioanalysis techniques of enzyme/substrate analysis and immunoassay show great promise for adaptation to FOCS. These techniques exploit the natural selectivity of the enzyme-substrate or antibody-analyte interaction. Many are naturally reversible, making them attractive for sensor applications.

Enzymes are catalytic proteins which react with varying selectivities to specific substrates. Enzyme reactions are reversible, and the enzyme is unchanged by the process. The reaction rates are often limited only by diffusion of the substrate to the enzyme (62). Enzyme-substrate interactions can be monitored by the changing fluorescence--arising from the native fluorescence of tyrosine, tryptophan, or phenylalanine residues in the protein--of the enzyme as the reaction progresses, but such changes are usually small, and the fluorescence signal is fairly weak. A more common approach is to monitor the signal from a colored product or reactant of the enzyme-substrate reaction. One application of this technique is the absorbance measurement at 404 nm of p-nitrophenoxide, the product of the catalysis by alkaline phosphatase of p-nitrophenyl phosphate (63). The fluorescence of NADH produced from NAD^+ during the oxidation of ethanol by alcohol dehydrogenase has also been used to monitor enzyme activity (64). An alternative arrangement is to immobilize a fluorescently tagged substrate. Reaction with an

analyte enzyme results in the release of the fluorophore and a change in the analytical signal (43). Other researchers have used enzyme methods to detect penicillin (20), bile acids (22), ATP (28), and glucose (26).

Immunological methods have become standard practice in clinical chemistry. Their specificity and sensitivity have made them very popular and a great number of in-vitro assay techniques have been developed for a variety of analytes. They are especially popular for biologically active compounds such as proteins and hormones. In light of this, one would expect to find quite a number of these assays adapted for use in FOCS. The actual number in literature is suprisingly small. These include several evanescent wave sensors described by Andrade (6) for immunoglobulins and insulin. Other evanescent wave sensors have been reported for the analysis of methotrexate (65), Immunoglobulin G (IgG) (65, 66), and human choriogonadotropin (hCG) (67). Sensors with a more conventional fiber optic sensing scheme have been developed for the analysis of a somewhat greater variety of analytes. These analytes include the small molecules (<5000 Daltons) phenytoin (68-70), theophylline, digotin, phenobarbitol (70), and benzo[a]pyrene (19, 40, 71-77). IgG seems to be the only protein molecule analyzed to date using conventional fiber optics techniques (78, 79).

Principles of Immunoassay

Some of the fiber optic sensors discussed in the previous section make use of immobilized antibodies as the reagent phase. These sensors are often called "immunosensors". Immunosensors differ from other chemical sensors in several ways. Many chemical sensors operate on the principle of rapid reversible reactions between the reagent and analyte. The reaction between antibodies and analytes is generally not considered to be reversible. The reagent and analyte in most chemical sensors are fairly small molecules and are less prone to problems associated with overcrowding of immobilized reagent molecules. A basic understanding of antibody structure and function is necessary to appreciate the particular advantages offered by immunosensors, as well as their limitations.

Antibody Structure and Function

Antibodies are large protein molecules that react specifically and noncovalently with antigen and hapten molecules. Antigens are relatively large (>5000 Daltons) molecules which elicit antibody production in animals. Haptens are smaller molecules that will elicit an immune response only when conjugated to larger molecules. Antigens and haptens have structural regions called epitopes that are recognized by antibodies and to which the antibody binds (80-82).

"Antibody" is a broad term referring to the function of any of the five classes of immunoglobulin molecules, IgG, IgA, IgM, IgE, and IgD. IgG is the smallest of these (molecular weight ~160,000 daltons) and the most abundant in human serum. IgG is usually represented as three structural units arranged in a Y shape (Figure 1.5). The molecule can be broken down into three portions, two antigen binding fragments ($F_{(ab)2}$) and a "crystallizable" fragment (F_c). The antigen binding portions contain the structural variations that allow the antibody to recognize specific antigen molecules. The F_c portion was once thought to be the same for all IgG molecules but is now recognized to have structural variations that seem to affect the molecule's biological activity. The IgG class is now considered to be made up of four subclasses of molecules whose functions are still being studied, but which seem to be independent of the antigen-binding function (83, 84).

Antibodies used in immunoassay techniques are produced in two ways. Polyclonal antibodies are isolated from the sera of immunized animals and are a mixture of antibodies specific to the same analyte antigen but with different affinities and recognizing different epitopes. Monoclonal antibodies are produced from fused cells (hybidomas) and are uniform antibodies that recognize a single epitope and have a single affinity.

Immunoassay techniques exploit the specific binding of antibodies with analytes. These techniques are among the most sensitive, selective, and widely applicable techniques for analysis

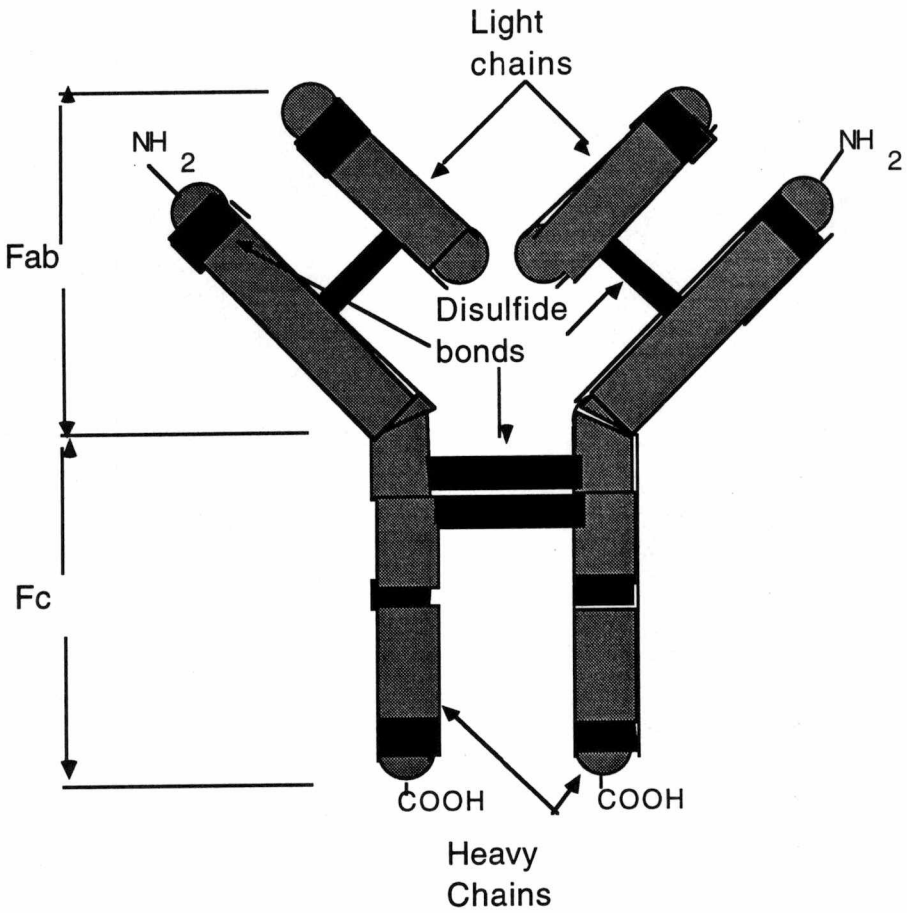

Figure 1.5. IgG Molecule.

of biologically active molecules. Specific antibodies can be generated for nearly any molecule, with monoclonal antibody technology making the commercial preparation of antibodies to very small molecules more feasible.

Techniques of Fluoroimmunoassays

A variety of detection schemes have been used for immunoassay. Radioimmunoassay, which uses isotope labels, was the primary clinical immunoassay technique for nearly 25 years. It has largely been replaced by nonisotopic methods such as enzyme-linked immunoassays and fluoroimmunoassays (85). Enzyme immunoassays use enzyme labels which react with a substrate, usually generating a colored product which is used to quantitate analyte concentration. Fluoroimmunoassays (FIA) employ a fluorescent tag and are detected using fluorescence spectroscopy. Some of the most common fluorescent labels for FIA are shown with excitation and emmision wavelengths in Table 1.1. Isothiocyanate derivatives of flurescein and tetramethylrhodamine B were used as labels for FIA in the research described herein. The isothiocyanate group aids in the covalent attachment of the label to the antibody.

Immunoassays are typically classified as homogenous or heterogenous, depending upon whether a separation step is necessary to remove free analyte (85). Homogenous FIAs require no separation step. When antibody binds to the analyte in a homogenous assay there is a change in a fluorescent property of either the antibody or

TABLE 1.1: Properties and Structure of some Fluorescent Labels.

Label	Structure	λex, nm	λem, nm
fluorescein isothiocyanate (FITC)	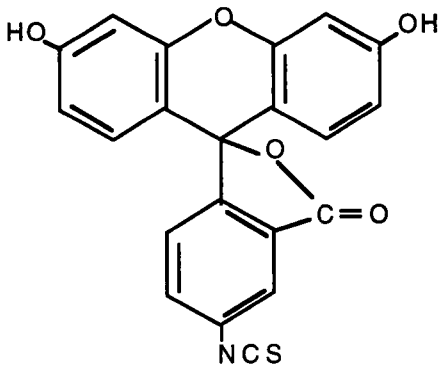	492	520
rhodamine B isothiocyanate (RITC)	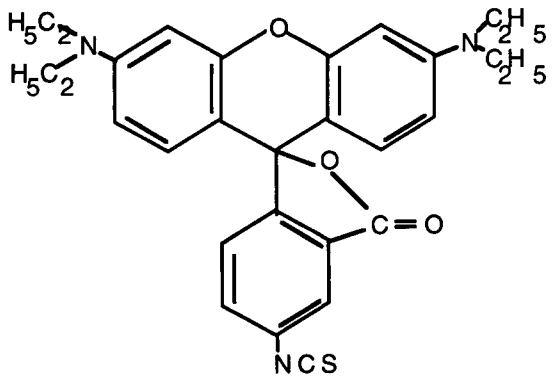	550	585
tetramethyl rhodamine B isothiocyanate (TRITC)	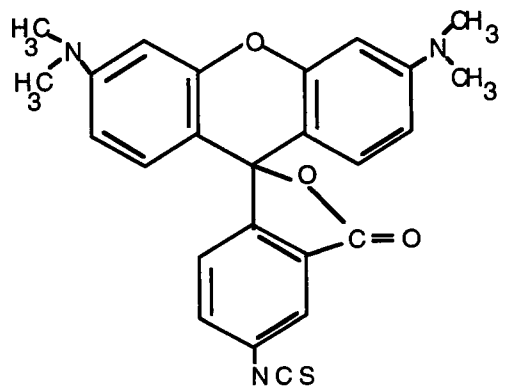	550	580
umbelliferones (coumarins)	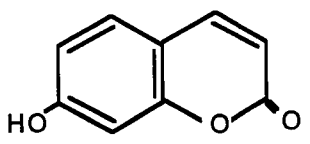	380	450

analyte. This is observed as a change in the polarization or fluorescence lifetime of a fluorescent label, or energy transfer between a fluorophore on the antibody and one on the antigen. These changes are used to quantitate the amount of bound analyte. Heterogenous FIAs require separation of unbound analyte from antibody-bound analyte. This is usually accomplished by immobilization of the antibody on a solid support. Unbound analyte is then rinsed free of the support. This allows direct measurement of flourescence intensity. The instrumentation involved in signal processing for homogenous assays is more complex than that used for heterogenous, but the homogenous assay usually requires fewer steps and is quicker. Measured changes in fluorescence polarization or lifetime for homogenous assays are usually very small, limiting the sensitivity of the technique.

Direct Assay

There are three categories of heterogenous FIA procedures (81). The procedure used depends upon characteristics of the analyte molecule. Naturally fluorescent molecules lend themselves well to the simplest procedure: direct FIA (Figure 1.6a.). In a direct FIA, analyte is incubated with an excess of antibody. After unbound analyte is rinsed away, the fluorescence signal is proportional to the analyte concentration.

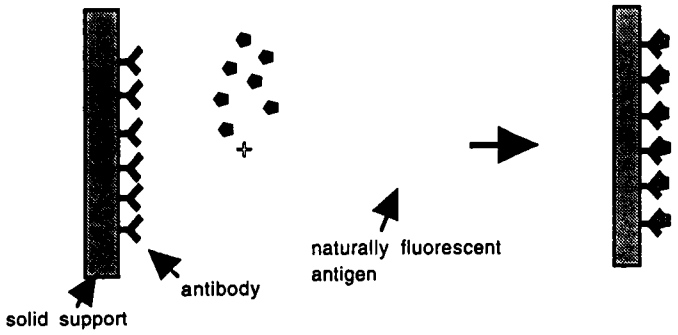

a. direct immunoassay

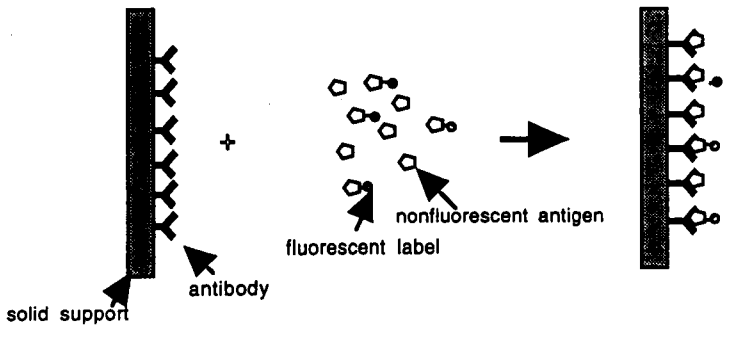

b. competitive immunoassay

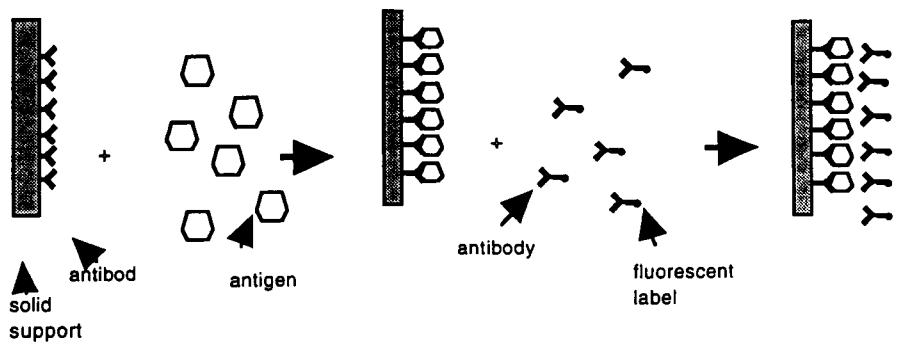

c. sandwich immunoassay

Figure 1.6. Types of heterogenous fluoroimmunoassays.

Competitive Binding Assay

Nonfluorescent analytes require either a competitive binding assay or a sandwich assay. In a competitive binding assay, fluorophore-labelled analyte competes with unlabeled analyte for binding sites on the immobilized antibody (Figure 1.6b.). The signal obtained after rinsing is inversely proportional to analyte concentration. This method requires that an equilibrium be established between the unlabeled and labeled analyte molecules. Linear dynamic range is usually fairly small (one order of magnitude of concentration) and relatively long incubation times are necessary to ensure that equilibrium has been established.

Sandwich Immunoassay

Sandwich assays are used for large analyte molecules (Figure 1.6c.). Antibodies to two different epitopes on the analyte molecule are employed. The first antibody is unlabeled and is usually immobilized on a solid support. This antibody concentrates or collects the analyte. The second antibody is labeled with a fluorescent tag and binds to a different epitope on the analyte, creating a "sandwich". Unbound antibodies and analyte are rinsed away and signal intensity is proportional to analyte concentration. The need for two distinct epitopes makes this technique applicable only to large molecules such as proteins. Signal for a sandwich assay is directly proportional to analyte concentration. Linear

dynamic range and sensitivity for sandwich assays are generally similar to those for direct assays.

CHAPTER 2

DEVELOPMENT OF A REGENERABLE FIBER OPTIC SENSOR

Introduction

One of the goals of FOCS research is the development of sensors that can be used for continuous or repetitive *in situ* monitoring. This type of sensor would have innumerable applications in medicine, industry, or environmental monitoring.

For a FOCS to be considered a "true" sensor--as opposed to a "probe"--one of the following conditions must be met 1) the interaction between analyte and reagent must be rapid and reversible, or 2) there must be sufficient reagent such that it is not depleted over long periods of time, or 3) there must be some means of regenerating the sensor, preferably in situ.

This researcher has approached the "continuous" sensor problem from each of these directions. Early experiments sought a sensor that utilized a reversible interaction between analyte and reagent. Later experiments approached the problem from the perspective of providing enough reagent for repetitive measurements with the same sensor. Recent research is centered around the development and use of a sensor that employs a regenerable or replaceable reagent phase. This chapter will be devoted to early research that resulted in sensor configurations that

did not meet the requirements for a regenerable sensor, but which provided valuable insight into the physical design aspects involved in a regenerable sensor.

In the course of these studies a number of different sensor configurations were used, but the basic experimental method used for antibody immobilization and the instrumentation for detection were essentially the same throughout the early research. These methods will be described in general terms in the next two sections; any variations will be noted in the more specific discussions of each sensor.

Development of Antibody Based Sensors with Sampling and Reagent Delivery by Diffusion

Antibody Immobilization Procedure

All of the following sensors involve immobilization of anti-rabbit IgG to some form of silica. The basic procedure was the same for all forms of the silica. The techniques for the procedure were adapted from protein immobilization procedures developed for affinity chromatography (86).

The silica is first derivatized with a cross-linking agent, glycidoxyproplytrimethoxysilane (GOPS) (Aldrich Chemical Co, Milwaukee WI). The silica was first etched for several hours in 1M NaOH at 40^{o}C, then rinsed with distilled water. The silica was then suspended in a 10% solution of GOPS in distilled water with the pH

adjusted to 3. The solution was stirred and heated for 3 hours, using dilute HCl and water to keep the pH at 3 and the volume constant. The silica was then dried overnight at 105°C.

A periodate coupling method was used to covalently attach the antibodies to the derivatized glass. The derivatized glass was incubated at room temperature in 0.025 N KIO_4 for 25 minutes. After rinsing with phosphate buffered saline (PBS) composed of 120 mM NaCl, 2.7 mM KCl, 10 mM Na_2HPO_4 in distilled water, with pH adjsuted to 7.4, the glass was incubated with antibody at 4°C for 24 hours. $NaBH_4$ solution was used to reduce any unreacted binding sites. An illustration of the steps in the derivatization process is presented in Figure 2.1.

The amount of antibody bound to the glass was determined by UV spectroscopy. The concentration of antibody before and after the incubation period was determined relative to a calibration curve at 280 nm. This allowed calculation of the amount of bound antibody. A similar method could be used to determine the amount of active antibody, measuring the concentration of an analyte before and after incubation with the antibody-silica.

Instrumentation

The instrumental apparatus for all of the sensors described below was essentially the same. Figure 2.2 illustrates the arrangement of the optical components of the system. An argon ion laser was operated at 488 nm (Cyonics/Uniphase, San Jose, CA,

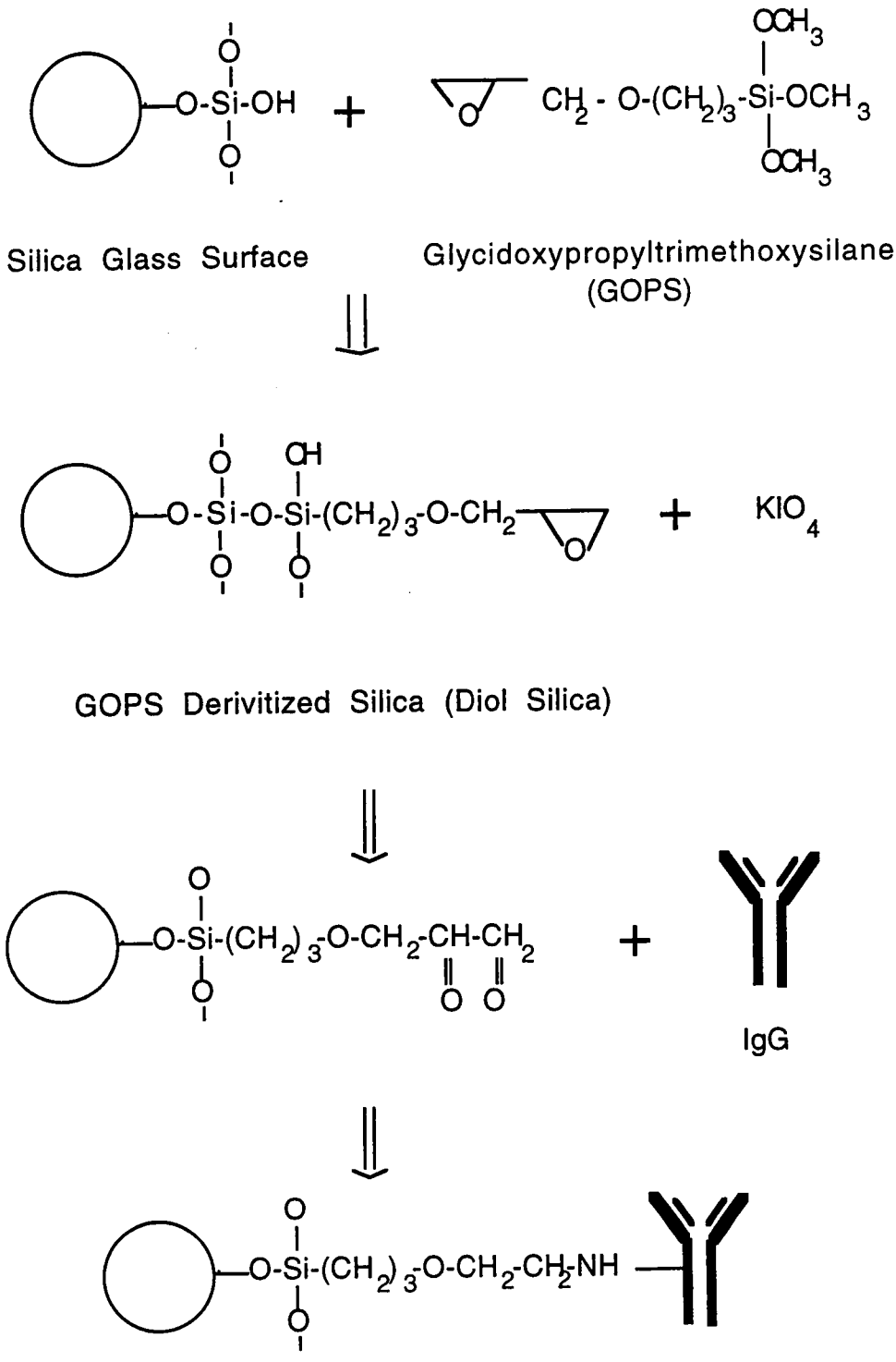

Figure 2.1. Immobilization of IgG on silica by periodate coupling method.

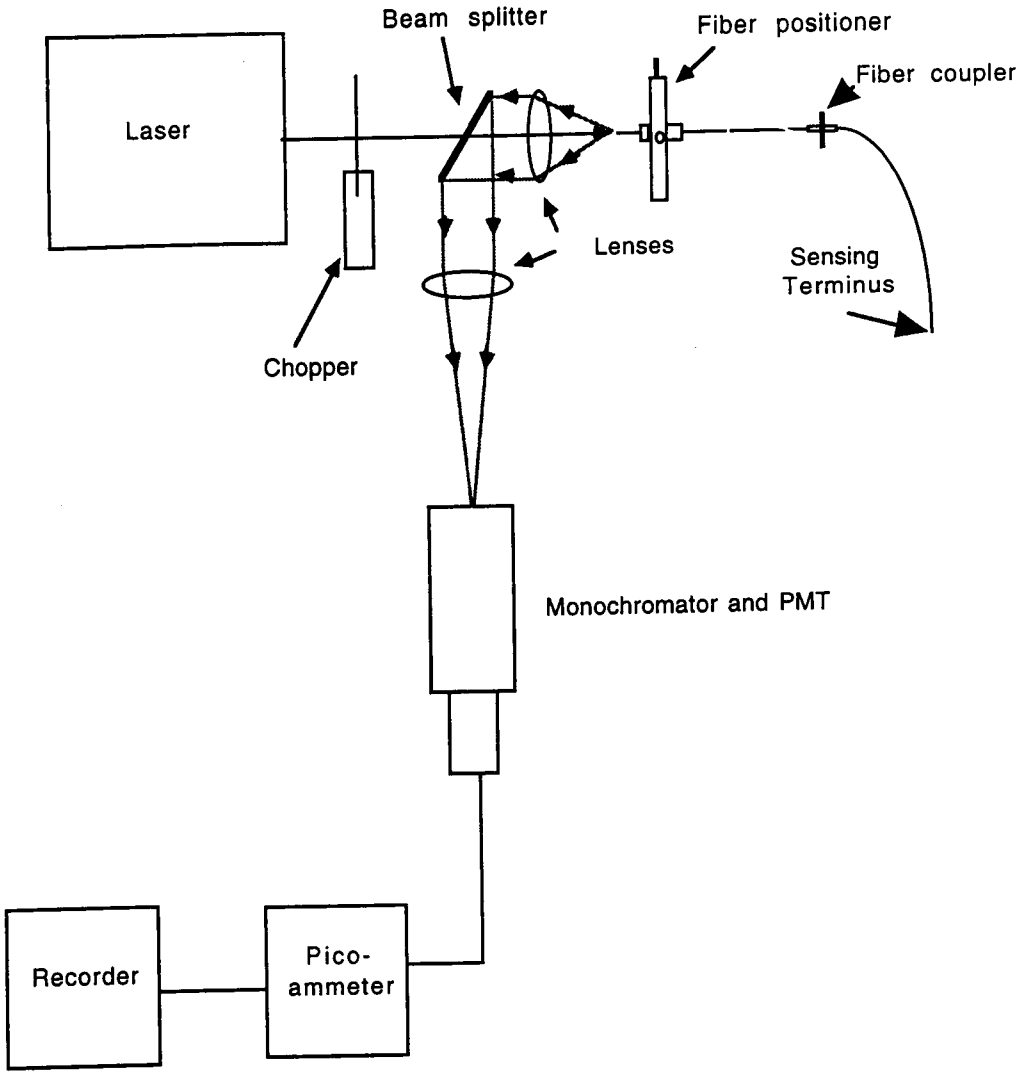

Figure 2.2. Optical arrangement for laser-based fiber-optic sensors.

Model 2001SL). A monochromator (Instruments SA, Edison, NJ, Model H10) with a 0.5 mm slit and a 488 nm bandpass filter (Corion Corporation, Holliston, MA) were used to isolate the fluorescence. A RCA 1P28 photomultiplier tube (Scientific Products, Atlanta, GA) was operated at 750 V. A picoammeter (Keithley Instruments, Cleveland OH, Model 485) was used to process the photocurrent. The resulting current was recorded using a strip chart recorder (Kipp and Zonen, Bohemia, NY). The optical fibers used in these experiments were 600 μm diameter fibers obtained from Math Associates (Westbury, NY). Optical fiber couplers were from Optical Fiber Technologies, Inc (Nutting Lake, MA). The couplers were polished to a mirror finish to reduce stray light and improve coupling efficiency. A fiber-optic micropositioner (Newport Electronics, Santa Anna, CA) was used to aid in focusing of the laser onto the optical fiber. The beam splitter was a dichroic filter (Corian Corporation, Holliston, MA) arranged at 45^{o} to the laser beam.

Five Prototype Sensor Designs

Capillary Sensor

This sensor used a configuration in which the fiber could see fluorescent reagents bound to capillary tubing within the field of view of the fiber.

Experimental. Anti-rabbit IgG (Sigma Chemical Co., St Louis, MO) was immobilized on round glass capillary tubing (Vitro Dynamics Co, Rockaway NJ) using the procedure described above. The tubing was then placed around a 600 μm optical fiber from which the cladding had been stripped for approximately 2 cm (Figure 2.3). The tubing was secured to the remaining cladding using Devcon Brand 5-minute epoxy (purchased at a local hardware store). The distance between the end of the optical fiber and the end of the capillary tubing was determined experimentally as follows. One batch of capillary tubing was reacted with FITC-labeled anti-IgG instead of plain anti-IgG. This gave a fluorescent coating on the inside of the tubing. A fiber was placed inside of the tubing but not secured with epoxy. The fluorescent signal from the fiber was then measured with different distances between the end of the fiber and the end of the tubing. The distance giving the maximum signal was determined to be approximately 5 mm.

For preliminary studies, the sensing end of the fiber assembly was filled with phosphate buffered saline (PBS) solution using a small gauge syringe needle. The sensor was then immersed in a solution containing rabbit IgG labeled with FITC (Sigma Chemical Co., St Louis, MO). This allowed monitoring of the diffusion of sample into the sensor and binding of the analyte to the capillary tubing. This was accomplished using the 488 nm line of the argon ion laser for excitation and monitoring the emission at 520 nm. Unbound analyte was rinsed by diffusion into PBS buffer solution.

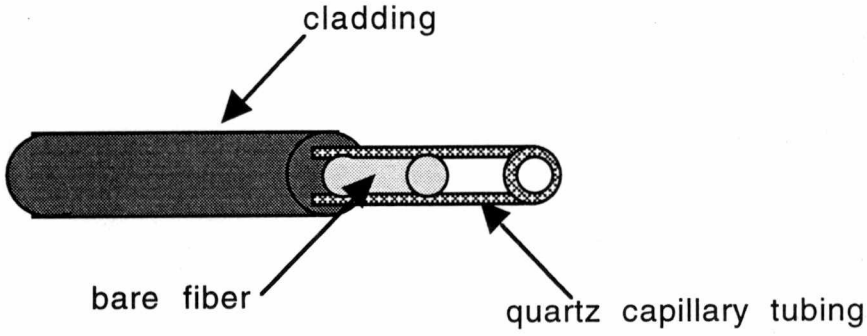

Figure 2.3 Capillary sensor. Antibody is covalently bonded to surface of capillary tubing.

The premise of the design was that analyte molecules (IgG) would diffuse into the sensor area and attach to the antibody. Second antibody, with a fluorescent tag, could then be introduced--also by diffusion--and bind to the analyte. Unbound analyte and antibody could be rinsed out using diffusion. The resulting fluorescent signal would be directly proportional to the amount of second antibody bound and thus to analyte concentration. The sensor could be regenerated using chaotropic reagents to break up the antibody-analyte bond.

Results and discussion. Results of the diffusion experiment are shown in Figure 2.4 . These results indicated that the diffusion time for sampling, rinsing and analyte introduction would be prohibitively long, requiring several hours for a single analysis. In addition, the signal from labeled IgG was very small and was superimposed over a large and noisy background signal. With such unpromising preliminary results, a new sensor design was sought.

Distal Face Sensor

This approach was a step backward to a simpler probe design. This design, like that of the capillary sensor discussed above, was essentially that of a one-shot probe, although regeneration might be achieved by use of chaotropic reagents.

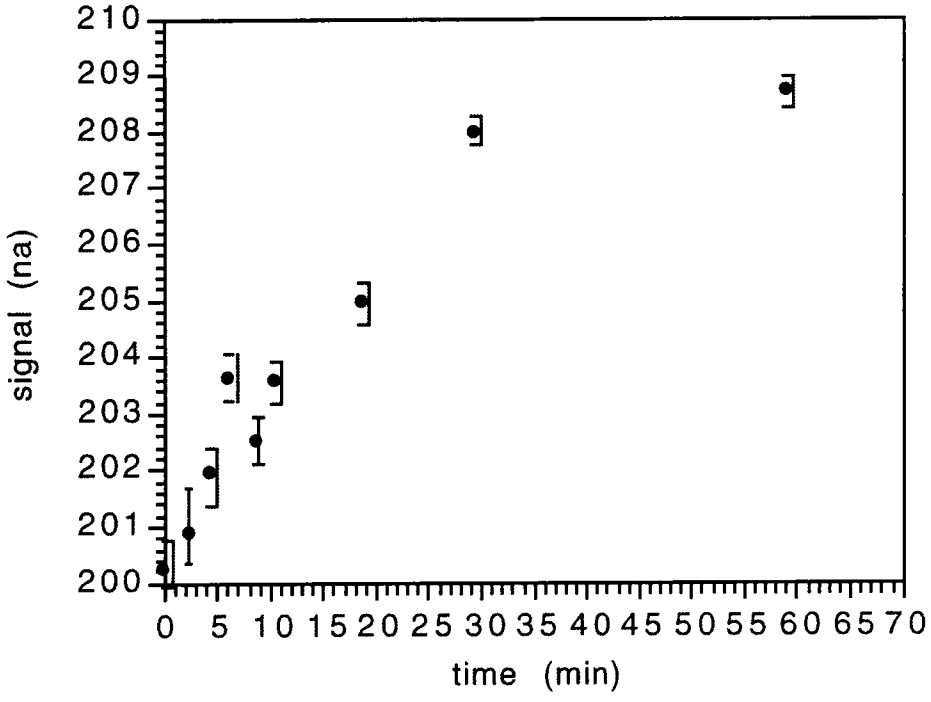

Figure 2.4. Diffusion of FITC-IgG into capillary sensor. Data points are average values for 4 sensors. Error bars indicate standard deviation of each value.

Experimental. In an attempt to circumvent the diffusion problem, anti-rabbit IgG was covalently bonded to the face of the optical fiber (Figure 2.5).

The fiber was placed in PBS solution containing 0.1mg/ml FITC-labeled rabbit IgG (FITC-IgG) and incubated for 2 minutes. Unbound analyte was rinsed away by dipping in buffer solution. The fluorescent signal was measured with the sensor in clean buffer solution. The same sensor was reimmersed in the FITC-IgG solution for an additional 2 minutes, rinsed, and the signal measured. This process was repeated until a maximum signal was reached in an attempt to determine the optimum incubation time for antibody-analyte binding.

This assay could easily be expanded to a sandwich assay by using unlabeled analyte and a labeled second antibody to the IgG.

Results and discussion. The results for five different fibers are reported in Figure 2.6. The signals obtained from the five fibers were very different, indicating irreproducible binding of antibody to the fiber and/or irreproducible light coupling to the fiber. This made it virtually impossible to develop a calibration curve since each fiber was essentially a one-shot device. In addition, the signal to noise ratio for each fiber was poor, with a small signal superimposed on a large and fairly noisy background. This was

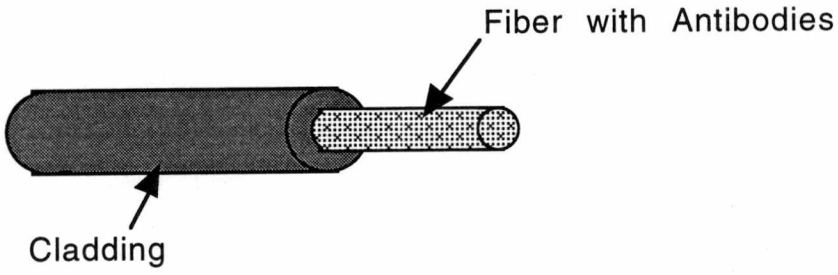

Figure 2.5. Bare Fiber with covalently attached antibodies.

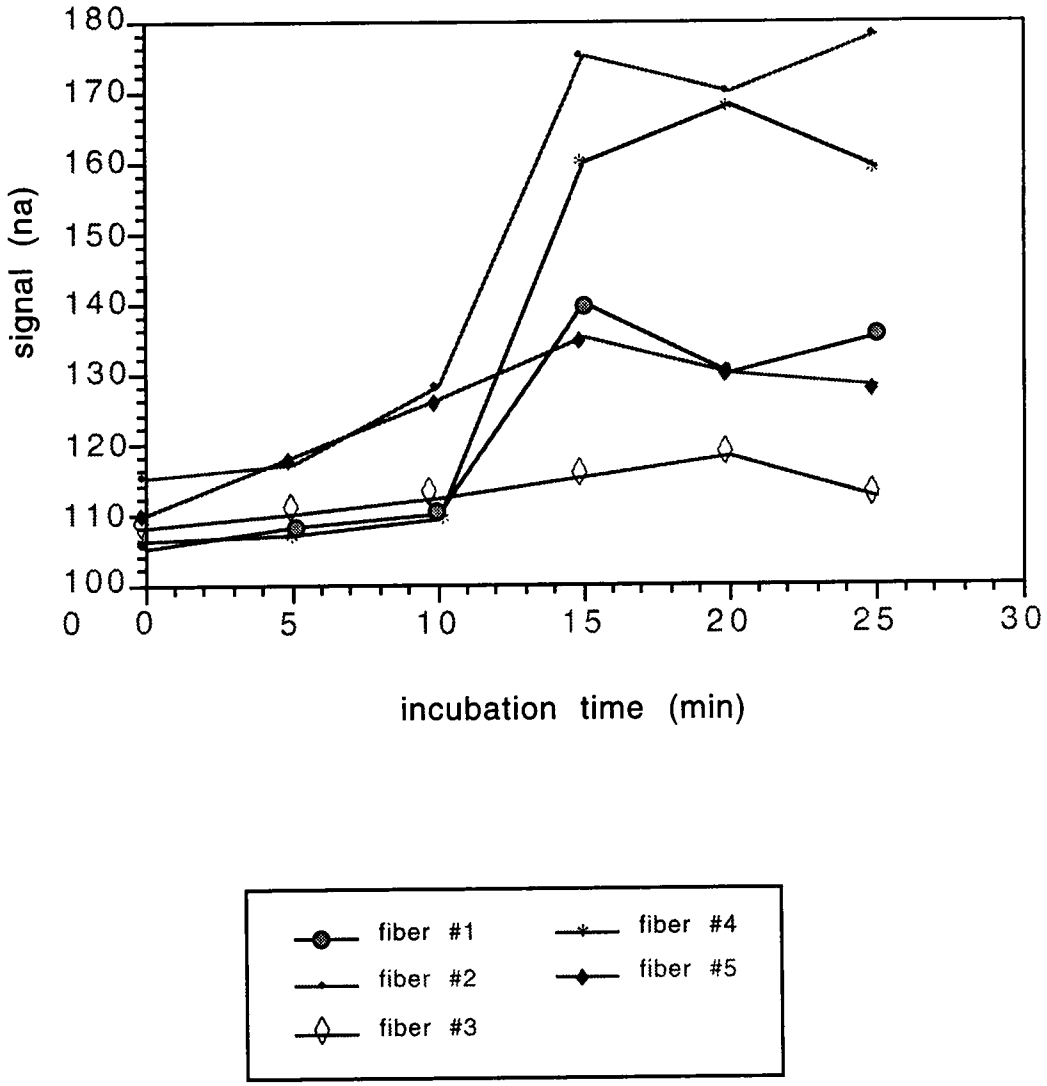

Figure 2.6. Comparison of signal at different incubation times for 5 fibers prepared with antibody bound directly to distal face of sensor.

believed to be caused by low antibody activity resulting in saturation of the probe with small amounts of analyte. The low activity was attributed to low coverage of antibody on the surface of the fiber due to the small surface area available for bonding. Attempts to increase the surface area of the fiber by etching with HF were largely unsuccessful; the slight increase in antibody binding was offset by increased noise, perhaps due to scattering, and the fibers became so fragile that they could be used only with great care--limiting the use to essentially one shot.

The distal face sensor offered the advantage of increased speed for the analysis relative to the capillary sensor, but this advantage was offset by the decreased surface area of the fiber face.

Bead Sensor

In an attempt to increase the surface area available for analyte binding, while providing reasonably rapid response, glass beads were immobilized in a single layer on the surface of the fiber (Figure 2.7).

Experimental. 75 μm diameter soda lime glass spheres (Duke Scientific, Palo Alto, CA) were derivatized with GOPS and dried as above, then affixed with epoxy in approximately a single layer to the tips of 600 μm optical fibers. This was accomplished by coating the end of a fiber with a thin coating of epoxy, allowing the epoxy to

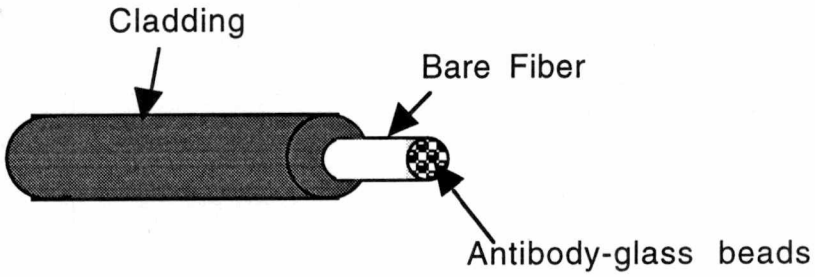

Figure 2.7. Bead sensor. Glass beads attached to fiber with water resistant epoxy.

set-up for several hours, then touching the fiber to a thin layer of the beads spread on a smooth surface. A water-resistant epoxy with a 24-hour cure time was used for this procedure after it was discovered that fast curing epoxy dissolved in the aqueous buffer used for the sensors. After the epoxy hardened the fiber was tapped gently to remove any unbound beads. Binding of the beads to the fiber could be observed by using a dissecting microscope to examine the end of the fiber. As controls, several fibers without beads (epoxy only) and fibers such as those in the previous section (distal face) were prepared and carried through the same procedures as those with beads. The fibers were then activated with periodate solution and incubated with anti-IgG as above. The fibers were incubated in 0.1mg/ml FITC-IgG solution for 30 minutes, rinsed, and the signal measured in PBS solution. This sensor design, like the previous one, could be expanded to a sandwich assay by using unlabeled IgG and fluorescently labeled second antibody to the IgG. Regeneration might be accomplished by use of chaotropic rinsing.

Results and discussion. Results of the above experiment are presented in Figure 2.8. It appeared that antibody and/or the analyte bound to the epoxy alone more strongly than to the bare fiber or the glass beads. It was suspected that the procedure used to activate the GOPS on the silica was also activating amine groups in the epoxy. Epoxy cement is composed of equal parts of resin and hardener. The resin is a low molecular weight polymer of Bisphenol

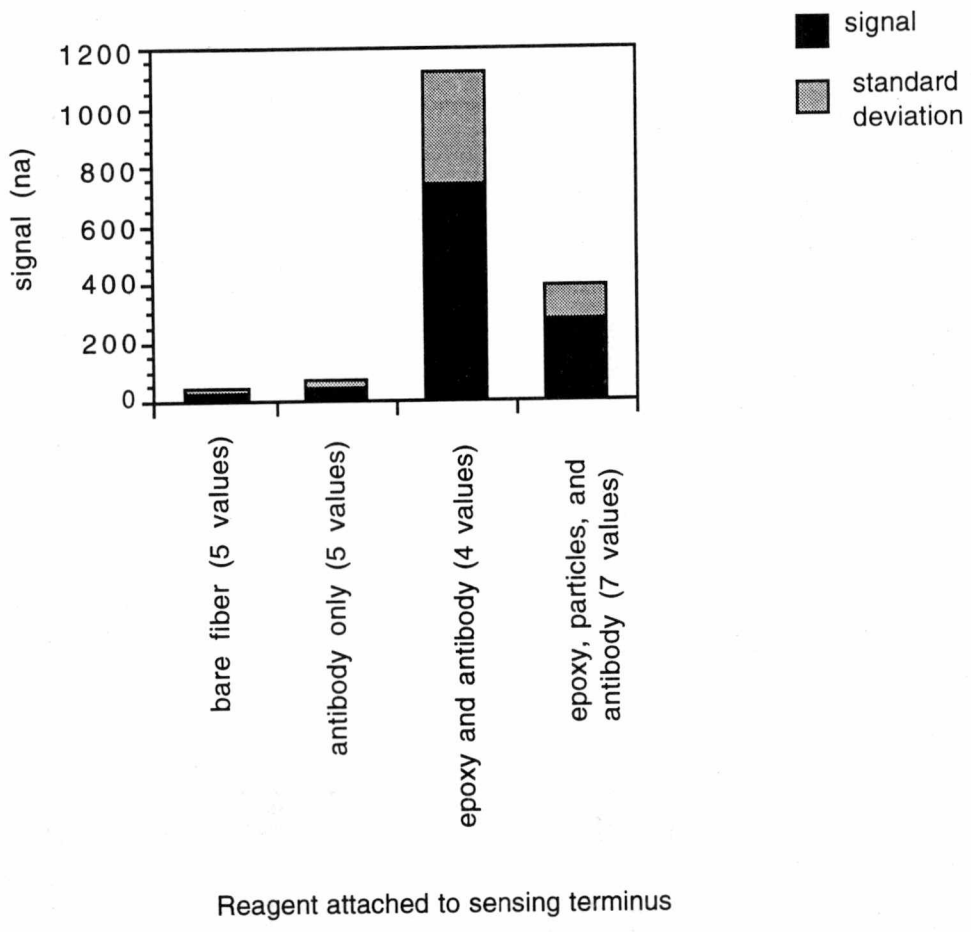

Figure 2.8. Comparison of average signal obtained from different sensing termini.

A and epichlorohydrin. The hardener is an amine such as $H_2NCH_2CH_2NHCH_2NH_2$ (93). It is possible that the amine groups in the hardener are also activated. Unfortunately the reproducibility was very poor, probably due to inconsistent coverage of the epoxy. Attempts to chaotropically rinse the fiber with epoxy and antibody with guanidine hydrochloride solution caused no drop in signal. Other activation procedures, including the use of a glutaraldehyde coupling procedure, were tried in an attempt to avoid activation of the epoxy, but there was no appreciable change in the signal from fibers prepared in this manner.

Inspection of the fibers with beads, using a dissecting microscope, showed a wide variation in the number of glass beads actually bound to each fiber. The range seemed to be from about 25 to more than 50 particles on the fibers. It was calculated that a single layer of closely packed beads would be about 64 beads on the surface of a 600 μm fiber. The signals from the individual fibers seemed to be proportional to the amount of beads on the tip, with a maximum signal occurring with about 30 particles fairly evenly dispersed over the surface of the fiber. This seemed to indicate that in addition to antibody bound to the epoxy, there was some antibody binding to the beads and that there was an optimum "packing" on the surface. Attempts to achieve reproducible binding of beads to the fiber were largely unsuccessful, as were attempts to regenerate the sensors using chaotropic rinsing.

It was decided to pursue another method for immobilization of the beads at the face of the fiber.

Fritted chamber sensor

This approach used a stainless steel chromatography frit as a chamber to contain beads at the tip of the fiber.

Experimental. Porous stainless steel frits with 5 μm pore size were obtained from Alltech Associates (Deerfield IL). The dimensions of the frits were 2.4 mm diameter and 1.8 mm thick. A hole 0.70 mm diameter and 1.6 mm deep was drilled into the frit in-house. Optical fibers could be inserted in the frit to a depth determined by the distance the cladding was stripped (Figure 2.9). After ultrasonication in PBS buffer to remove air bubbles, the frit was filled with a slurry of the 75 μm beads (no antibody) in PBS buffer. The tip of an optical fiber was inserted into the frit to a depth of 1.0 mm. The frit was then affixed to the fiber with epoxy. After the epoxy cured, the signal from the PBS and blank beads was measured. The sensor assembly was then immersed in a 10^{-5} M FITC solution overnight to determine if diffusion into the frit would occur. When essentially no diffusion occurred, it was suspected that the frit might still contain air bubbles. To clear air bubbles from the frit a chromatographic column filling apparatus was used to force buffer into the pores of a frit. The frit was then assembled with the fiber and beads as before. The signal with excitation at 488 and

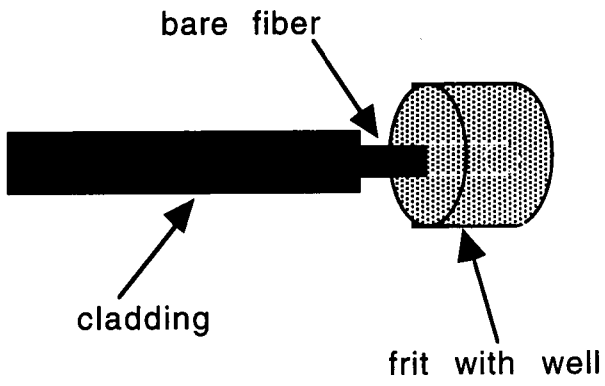

Figure 2.9. Fritted chamber sensor.
Glass beads trapped in well.

emission at 520 was monitored intermittently for several hours while the sensor was immersed in FITC solution.

Results and discussion. Results of the experiment to measure diffusion into the sensor are presented in Figure 2.10. These data show that diffusion did occur into the frit after solution had been forced into the pores. The rate of diffusion was very slow, with the signal rising very slowly over a 3 hour period and never reaching a stable maximum. Diffusion out of the frit was also very slow, with a return to 25 % of background signal only after 4 hours. Diffusion times of this length would not be practical for sensor applications, since analyte concentration might change greatly during the analysis time.

Examination of the frits using a dissecting microscope revealed gross irregularity near the top of the chamber, with many pores seemingly occluded by metal filings during the drilling process. It was assumed that the frit was similarly damaged nearer the bottom of the well, in the area where diffusion should be occurring. Such technical difficulties precluded further investigations with the fritted chamber until a better drilling method became available or until such frits became commercially available. Another method for creating a chamber at the end of the fiber was sought.

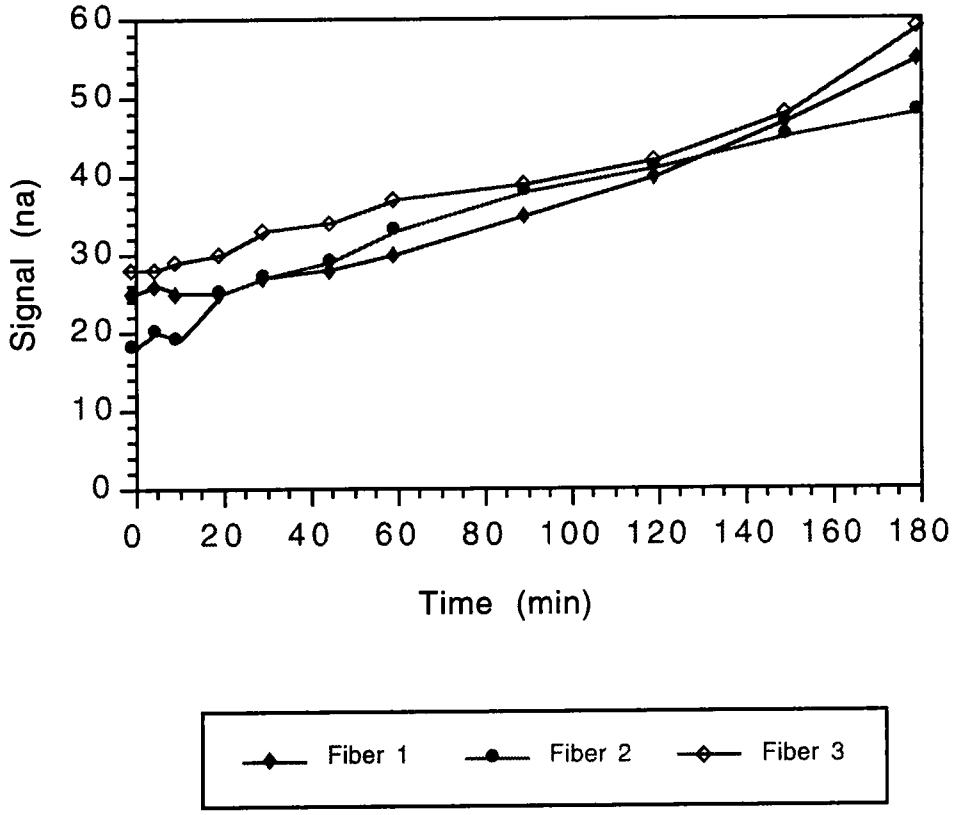

Figure 2.10. Diffusion of FITC into fritted sensor. Fibers 1, 2, and 3 were prepared using three different frits from the same lot.

Membrane Sensor

This sensor design utilized confinement of antibody-beads behind a semi-permeable membrane. It was similar in design to the sensors reported by Tromberg, et al (40, 72, 87). These sensors used a "fast membrane" with a 10,000 molecular weight cut-off (MWCO) and free antibody confined inside the sensor to detect benzo (a) pyrene. Such a design is not possible for large molecular weight molecules such as proteins where the molecular weight of the protein and antibody are similar. Use of a membrane with a large MWCO requires confinement of the antibody on a much larger surface or substrate inside of the chamber.

Experimental. Figure 2.11 illustrates the sensor configuration. Heat-shrink tubing was used to create a cylinder that would fit around the cladding of a 600 μm fiber. A membrane was stretched across one end of the cylinder and secured with heat-shrink, creating a chamber. The assembly was also large enough to fit around the end of a 16 gauge syringe needle. This allowed solutions to be introduced to and rinsed from the tip independently of the fiber apparatus. A slurry containing antibody-beads could be introduced using this feature. A stop on the optical fiber kept the membrane 0.5 mm from the tip of the fiber. The probe tips were secured to the optical fiber with heat-shrink tubing.

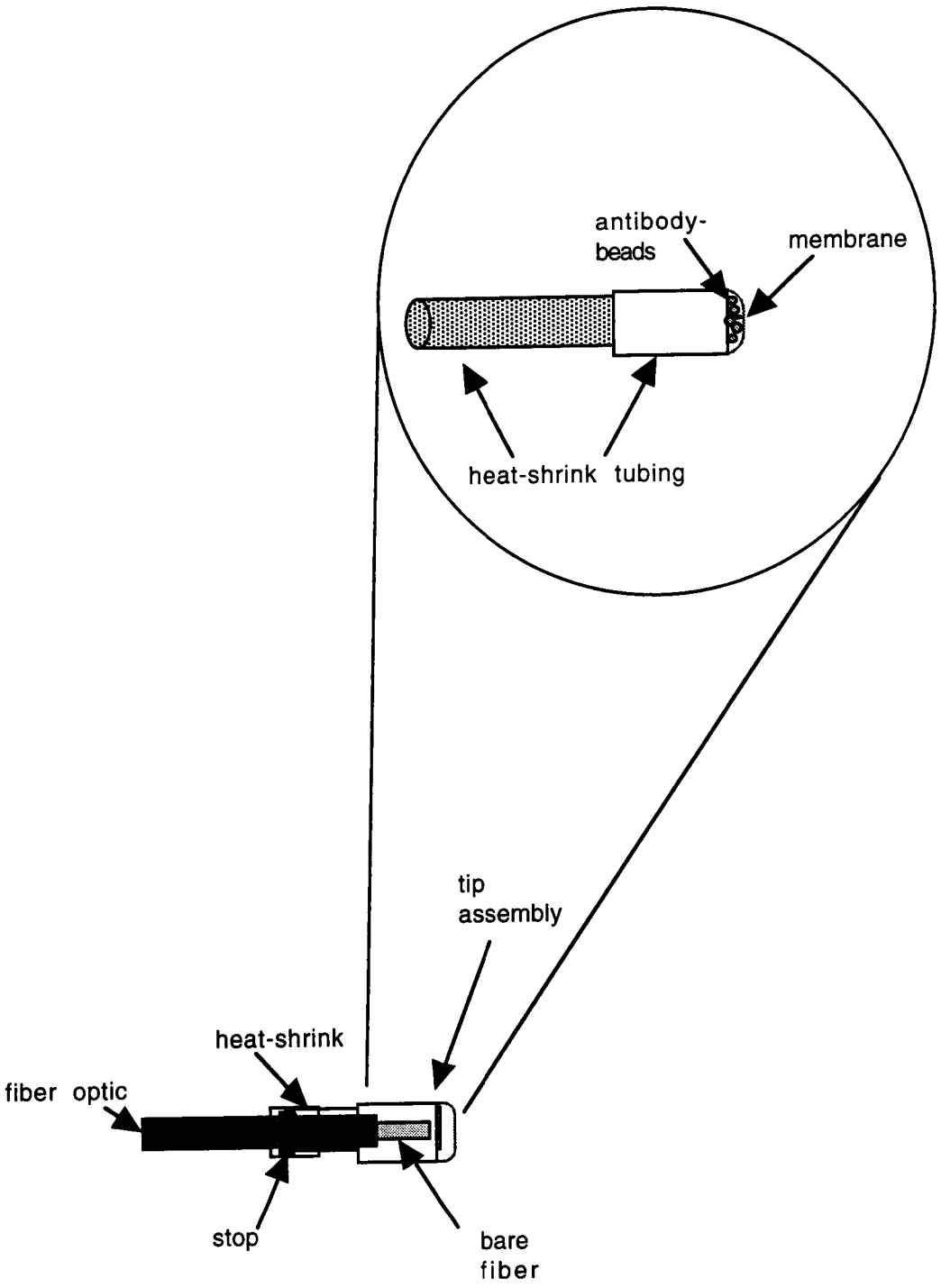

Figure 2.11. Membrane sensor. Enlarged area shows tip assembly.

Polycarbonate, cellulose ester, and polyester membranes (Spectra-Por Brand, purchased from Scientific Products, Atlanta, GA) were tested for permeability to FITC-IgG by monitoring the diffusion into the sensor. Pore sizes of the membranes ranged from 1 to 10 μm. In addition, Teflon membrane with a 1,000,000 MWCO was tested. The optical apparatus was as described above except for the omission of the optical fiber coupler. Reproducibility problems with the couplers led to the use of a single long fiber coupled directly to the laser beam. Replaceable tips made this a practical design, since the same optical fiber could be used repeatedly without realigning the laser beam. When it was necessary to replace the fiber, the laser could be aligned without the sensing tip in place, making alignment an easier process.

This sensor design also allowed mild aspiration to be used to draw solutions into the sensor. This was accomplished by sliding the tubing along the fiber to enlarge the chamber--creating a vacuum that drew solution into the sensor. Compression of the chamber forced solution out through the membrane. Vacuum grease was used to lubricate the tubing and to create a seal so that solutions flowed through the membrane only. Several of the membranes were tested for permeability by aspiration.

Results and discussion. Figure 2.12 summarizes the results of the diffusion sampling and aspiration sampling experiments. From

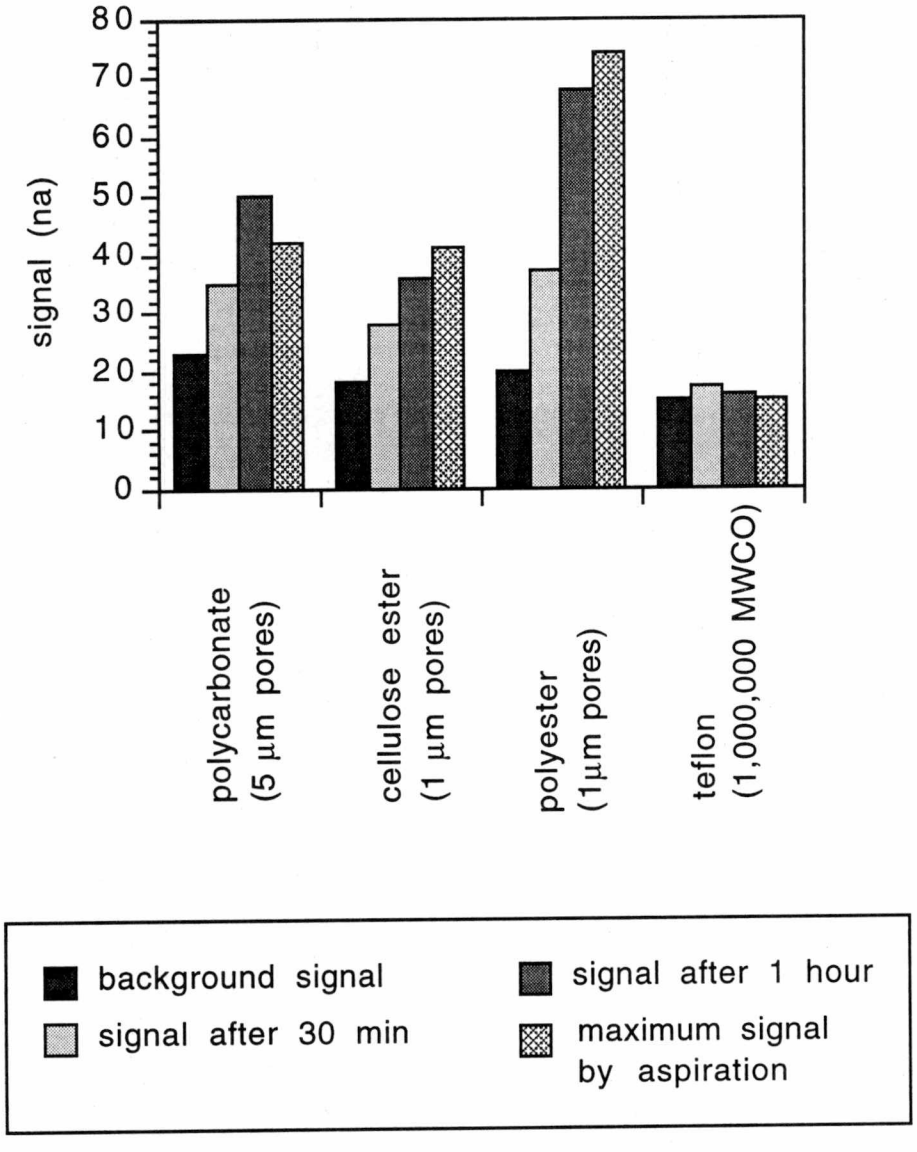

Figure 2.12. Diffusion and aspiration data for membrane sensor. Data are for single runs with one fiber, sensor tips interchanged to change membranes.

the data it was clear that diffusion would not be a valid sampling method for this type of sensor. For most of the materials, one hour incubation resulted in a signal that had not leveled out, indicating that equilibrium had not yet been reached. The polyester membrane appeared to come closest to achieving equilibrium; the signal for this fiber had changed only about 2 percent in the 5 minutes prior to the one hour incubation time point that was plotted. Data were not collected for longer than one hour since the goal of the research was to attain sampling times that were practical for use in repetitive measurements.

Some of these results may be in part attributed to the nature of the membranes tested. The Teflon membrane was not very compatible with aqueous solution. It was fairly hydrophobic, making it difficult to wet the membrane so that diffusion could occur. In addition, the tortuous path design of the pores made this membrane more suitable for its original purpose which was separation of large molecules from solutions. It was never intended that large molecules pass through the membrane readily. The same could be said for the cellulose ester membrane which also was a tortuous path membrane. However, the pores in the membrane were much larger than the size of the IgG molecule, and the membrane material was more compatible with aqueous solution. The polycarbonate and polyester membranes had straight pore structures. The polyester was actually a woven fabric. The polycarbonate membrane was extremely brittle compared to the other materials, especially if

allowed to dry. This very thin membrane gave a much higher background signal, indicating that the fiber could "see-through" the membrane and was detecting fluorophores not in the sensing chamber. On the whole the polyester membrane showed the most promise, giving the highest overall response and the best aspiration response.

The aspiration data indicated that aspiration might be a valid method for sampling. When a slurry of antibody beads was added to the sensor, however, the signal following aspiration became completely irreproducible and extremely noisy. The noise in the signal changed from a variation of one to two nanoamps before aspiration to as much as 100 na after aspiration. This was attributed to movement and perhaps even loss of the beads within the field of view of the fiber. Some method was needed to hold the beads in place while aspirating in the sample and any other reagents necessary for the analysis.

The membrane confinement approach still seemed to be the most promising. Filling a sensor tip with a slurry of pre-reacted beads (containing antibody and FITC-IgG) gave a signal of about 300 na over a background of around 15 na for the sensor filled with antibody beads only. This signal to noise was the best of any of the previous sensors except for the sensor with beads attached to the tip which was plagued by irreproducibility.

Regenerable Sensor with Active Reagent Delivery System

Slow diffusion rates into and out of the previous membrane sensor made it clear that a sensor capable of performing sandwich assays would require some other means of reagent introduction and rinsing. Sandwich assays require several rinsing steps and the delivery of second antibody.

Sensors were developed which used chromatography columns to deliver reagents to a sensing chamber. Several designs were tested using different column configurations and sensing chambers. Early models of this sensor were used for sampling by diffusion. Later modification allowed for sampling by aspiration.

Sensor Design and Construction

Two basic sensor designs were used for a membrane sensor. Detailed descriptions of the construction of these devices have been published (88). A brief description is included here for clarity.

In the first sensor design, four 200 μm id, and two 320 μm quartz capillary columns (Polymicro Technologies, Phoenix, AZ) were arranged symmetrically around a 400 μm optical fiber (General Fiber Optics, Cedar Grove, NJ) and held in place using epoxy. An in-house made template aided in arranging the columns and fiber and holding them in place while the epoxy hardened. Once the epoxy had cured, the fiber/column bundle was polished to an even, mirror-smooth surface using an apparatus designed for polishing optical fiber

couplers. The 320 μm columns had been tapered at the ends to accommodate small pieces of frit material which were held in place with 200 μm columns secured behind the frit material in the columns with epoxy. In the other sensor design, the 320 μm columns were replaced with 200 μm columns. Figure 2.13 illustrates the fiber/column bundle.

To increase the flow rate of solutions in the second sensor design, two capillary columns with diameters of 320 μm and two with 520 μm diameters were spliced onto the 200 μm columns near the sensor tip. The 520 μm and 200 μm columns were paired and terminated with 16 gauge syringe needles. One of the 320 μm leads was terminated with a syringe needle, the other with a short length of 16 gauge needle tubing and a Rheodyne ferrule. This fitting allowed the sensor to be connected to an HPLC injector (Rheodyne, Model 7010, Alltech Associates, Deerfield IL) for delivery of antibody-bead slurry. The needles could be sealed off with syringe valves (Mininert, Scientific Products, Atlanta, GA), so that the flow into and out of the sensor could be controlled. A syringe pump (Sage Instruments, Cambridge MA) was used with different sizes of disposable syringes to control the flow rate of solutions into the sensor tip. The 520 μm columns were used as outlets, the single 320 μm column was for rinse solutions, and the 200 μm columns were used for reagent delivery and for aspiration of sample. Figure 2.14 illustrates the entire sensor assembly, including a "T" assembly used for aspiration sampling.

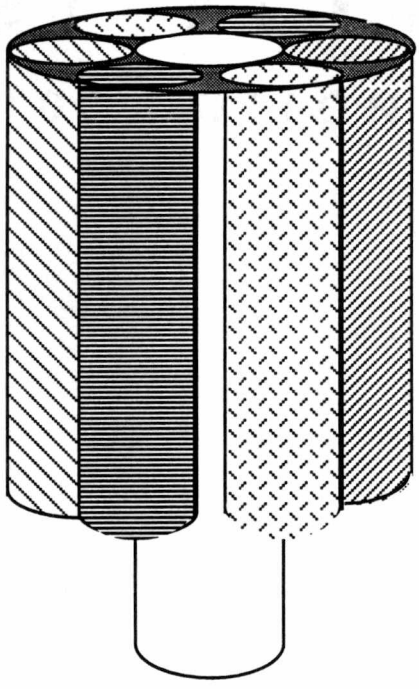

Aspiration and sample introduction
Rinse and flush inlet
Outlets (fritted in first design, open in second)
Bead inlet
Fiber optic

Figure 2.13. Fiber/column bundle.

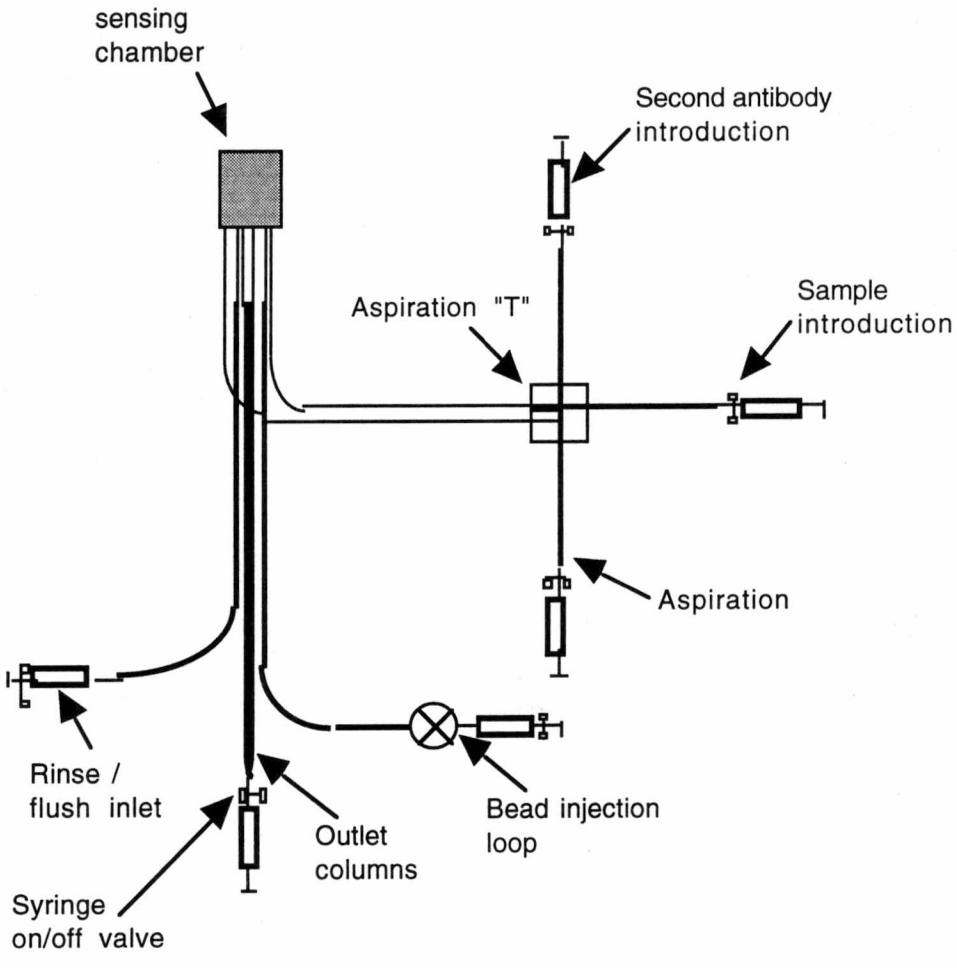

Figure 2.14. Fiber optic sensor assembly.

The first sensor design was intended to allow retention of the solid phase reagents inside the sensing chamber during aspiration sampling. Aspiration would occur through the fritted columns, resulting in the reagents being held against the frits. Subsequent delivery of rinse solution through the same columns would redistribute the packing material inside the sensing chamber. Preliminary studies with this design, and a membrane sensing chamber similar to that described above, indicated that the beads became tightly packed against the frit material whenever solution was passed through the columns. This forced the beads out of the field of view of the fiber. Addition of more beads in an attempt to fill the entire sensing chamber with beads compounded the problem by restricting flow. No amount of rinsing would dislodge the beads, leading to mechanical failure of the sensor.

This sensor design was abandoned in favor of the second design which required that all reagents be delivered with solution flow out of the sensing chamber through the membrane or frit. This kept the beads in position against the end of the sensing chamber, inside the field of view of the fiber.

Membrane Sensor

Experimental

Using the fiber column bundle described above, the sensing chamber for this sensor was a modification of the membrane chamber described previously (page 50) and illustrated in Figure 2.11. Heat-shrink tubing was used to form the chamber and secure the membrane but epoxy was used to secure the heat-shrink to the fiber/column bundle. This assured a good seal around the top of the chamber, an important consideration since solutions would be delivered under pressure. Two different pore sizes of polyester (1 μm and 5 μm) and polycarbonate membranes (1 μm and 5 μm) were tested using this design.

Preliminary tests were performed to determine flow characteristics of the sensing chamber before the addition of bead slurry. These tests used dilute FITC solutions to determine the maximum flow rate possible for reagent delivery with each membrane. It was determined from these experiments that reagent delivery times would be prohibitively slow with the 1 μm membranes of either material. Flow rates of greater than 5 μl/min caused the membranes to "blow-out". The 5 μm pore size membranes allowed flow rates of 10 - 15 μl/min.

Immunobeads (antibody bound to silica) were prepared in the manner described above. For these experiments anti-IgG was bound to 10 μm Spherisorb silica chromatography media (Alltech

Associates, Deerfield IL). Some of the immunobeads were pre-reacted with FITC-IgG to create a fluorescent signal that would allow monitoring of the beads as they were injected into the sensor tip. Two different concentrations of pre-reacted bead slurries were injected into the sensor using different injection loops to control the volume. The purpose of the study was to determine the optimum injection volume and slurry concentration. Conditions were sought that gave a large signal but also allowed complete flushing of the beads from the sensor in a reasonable time.

Once an optimum bead concentration and injection volume were chosen, reproducibility of slurry injection was studied with repetitive injections of pre-reacted immunobeads. During these experiments the polycarbonate membrane proved to be too brittle for repetitive injections; in addition it seemed to suffer from see-through effects and was thus ruled out for further investigation.

Blank silica beads (no antibody) were injected into the sensor. FITC solution was flowed past the beads, then rinsed out, to characterize the rinsing characteristics of the sensor.

Diffusion of solutions into the sensor, both with beads and without beads in the sensor, was tested with 10^{-4} M FITC and with 0.5 mg/ml FITC-IgG .

Sampling by aspiration was also studied. Results from earlier experiments indicated that aspiration after the beads were in place would cause irreproducible and noisy signals, perhaps due to loss of the beads from the field of view of the fiber. This sensor design

allowed aspiration of the sample into a "holding" column before introduction of the immunobeads into the sensor. The beads could then be held in the sensor tip while the sample was reintroduced. Rinse solution could then be introduced behind the sample to insure complete delivery of sample. A "T" design attached to the aspiration column allowed control of the amount of sample delivered. Mild aspiration on one lead of the "T" pulled solution through the sample tip and into the 200 μm column(s) leading to the "T". Continued aspiration filled the "T" with sample solution. Rinse solution was then delivered from another lead in the "T". This allowed delivery of a reproducible volume of aspirated sample, since the volume from the tip of the sensor to the "T" was constant. Reproducibility of aspiration was studied with FITC and FITC-labeled IgG. Aspirated samples were expelled into 1 ml volumetric flasks with enough rinse solution to return the signal inside the sensing chamber to baseline (~50 μl). After dilution to the mark, the absorbance of the solutions at 488 nm was used to determine the concentration of FITC and FITC-IgG. Comparison to a calibration curve for fixed volumes of the fluorescent solutions dissolved in 1 ml of buffer, allowed determination of the sample volumes.

Results and Discussion

The results of varying slurry concentration and injection volume are presented in Figure 2.15. From these data it was determined that a 50 μl injection of 10 mg/ml slurry gave the best

a.

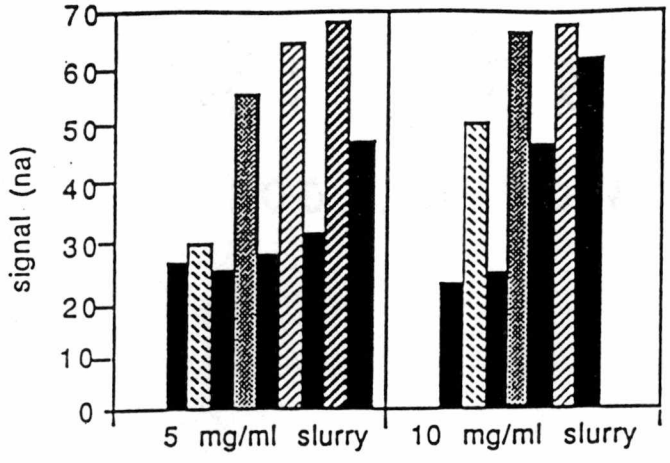

b.

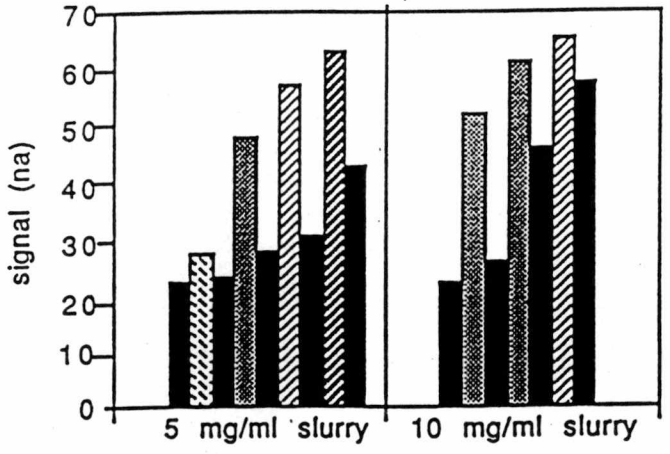

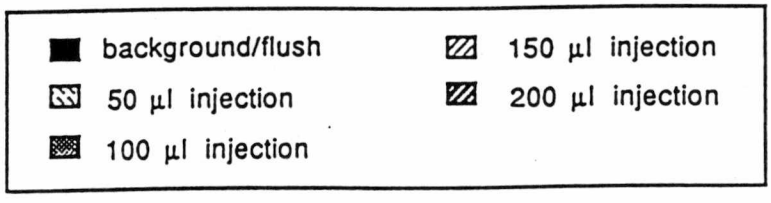

Figure 2.15. Injection of Immunobeads. Signal from different bead densities and injection volumes (a) 5 µm pore size polyester membrane, (b) 5 µm pore size polycarbonate membrane.

combination of signal, flushability, and time required for injection. The 100 and 150 µl injections required multiple injections from a 50 µl injection loop, while the 200 µl was a single injection, but would not flush out, due perhaps to packing of the beads into the sensing chamber. Because the membrane would allow flow rates of only 10 -15 µl/min, at least 5 min was required just to deliver 50 µl of slurry into the sensor tip.

Table 2.1 summarizes the results of the reproducibility of injection for beads that had been reacted with FITC-IgG. Reproducibility in a single sensor was fairly good (CV<10 %), but sensor to sensor reproducibility was essentially nonexistent. Each new sensor tip gave a different signal from the same injection volume of beads. This was thought to be caused by variation in the sensor volume and flow characteristics.

Table 2.2 summarizes the results of the experiments to determine rinsing, diffusion, and aspiration characteristics of the sensor. These data seem to indicate that the rinsing characteristics of the sensor were rather poor. The beads injected for this study had no antibody on them and should not have bound FITC (previous attempts to force binding of FITC to silica had been largely unsuccessful). The signal did not return to background until the entire sensor was flushed out with rinse solution. Because the flush signal returned to background it was assumed that the FITC was not sticking to the membrane, but was being trapped elsewhere in the sensing chamber.

Table 2.1 Reproducibility of immunobead injections for three different membrane sensors constructed with 5 μm pore size polyester membrane.

Measurement	Sensor #1		Sensor #2		Sensor #3	
	inject (na)[a]	flush (na)[b]	inject (na)[a]	flush (na)[b]	inject (na)[a]	flush (na)[b]
1	750	15	565	16	658	12
2	788	17	578	18	649	14
3	765	19	583	18	667	14
4	774	19	549	22	639	16
5	758	21	570	26	647	18
average	767	18.2	569	20	652	14.8
CV	1.9	12.5	2.3	20	1.7	15.4

Notes:

a. 50 μl of 10 mg/ml immunobeads, batch reacted with FITC-IgG. Injection accomplished using 50 μl injection loop followed by approximately 200 μl of rinse solution.

b. Sensor flushed out with water until stable signal attained, usually about 0.5 ml of rinse solution required

Table 2.2 Signal and Reproducibility data for isolated steps in membrane sensor constructed with 5.0 μm polyester membrane.

Measure-ment	Back-ground signal (na)	Delivery of blank beads (na)[a]	Rinse signal (na)[b]	Delivery of FITC (μa)[c]	Rinse signal (na)[b]	Flush signal (na)[d]	Diffusion of FITC --signal after 20 minutes (na)[e]	Diffusion of FITC-IgG -- signal after 20 minutes (na)[e]	aspiration of FITC signal(μa)/ volume aspirated (μl)[e]	aspiration of FITC-IgG signal(μa)/ volume aspirated (μl)[e]
1	5.0	50.5	50.4	2.5	154	7.0	10.0	9.8	3.0/15.1	2.5/14.2
2	6.0	48.6	48.0	2.4	159	6.3	9.4	10.2	3.1/15.2	2.6/14.5
3	5.0	49.3	49.2	2.8	155	5.8	9.8	9.2	2.9/ 14.9	2.3/ 14.1
4	5.5	55.4	55.0	2.7	161	7.5	10.5	10.4	3.2/ 15.0	2.8/ 15.0
5	5.8	46.5	46.9	2.3	158	6.8	9.5	8.1	3.3/ 15.1	2.2/ 14.5
average	5.7	50.1	49.9	2.5	157	6.7	9.8	9.5	3.1/15.1	2.5/14.5
CV	7.4	6.6	6.3	8.3	1.8	9.8	4.5	9.7	5.1/0.75	9.6/2.4

Notes: See experimental section for more detail

a. 50 μl of 10 mg/ml, 10 μm diameter blank silica beads

b. 100 μl of water delivered to sensing chamber via rinse inlet leads

c. 50 μl of 10^{-4} M FITC delivered to sensing chamber with blank beads in place

d. Sensor flushed out with water to remove beads and remaining FITC

e. FITC concentration = 10^{-4} M, FITC-IgG concentration = 0.5 mg/ml. Volume measured by expulsion of aspirated sample and dilution to 1ml. Absorbance of this solution was measured and compared to a calibration curve derived using fixed volume of "sample" solutions diluted to 1ml

Results from the diffusion experiment indicated that neither FITC nor FITC-IgG diffused into the sensor in a measurable amount after 20 minutes. In another experiment, a sensor was left overnight in FITC solution. This resulted in an increase in signal of about 8 na over the background signal.

Aspiration proved to be a much better method of sampling; however, these data are reported for a sensor with no bead slurry in the sensing chamber. Because of the poor results of the rinsing experiment, it was determined that attempting to measure the amount of solution aspirated by passing the solution over slurry until the signal returned to baseline would be an impossible task.

The sensor allowed control of aspiration volume by changing the length of the columns leading to the "T". The CV's for aspiration signal and volume aspirated were not the same. CV's for the signal were larger, indicating that the signal might not accurately reflect the volume aspirated. CV's for the aspiration of the labelled IgG were slightly larger than those for the smaller FITC molecule. This may have been due to adsorbtion of the protein to the membrane, or resistance by the membrane.to the aspiration of the larger molecule

These preliminary experiments illustrated that the mechanics of the sensor design were workable and revealed some important considerations in using the sensor. In addition these experiments illustrated some much needed improvements. Rinsing characteristics

needed to be improved, as did problems with sensor to sensor reproducibility.

These experiments revealed that any air bubbles in the system would cause problems with reproducibility of injections and aspiration. It was crucial that all bubbles be removed from the sensor during a conditioning period. The presence of air bubbles in the sensor after previously bubble-free operation indicated a leak in the sensor, frequently at one of epoxy joints, or in one of the syringe valves. Failure of the membrane was a major problem, resulting in the need to "recalibrate" the sensor with a new membrane tip. This meant verifying that a 50 µl injection of batch beads gave a reasonable and reproducible signal.

Reproducibility of antibody binding to the immunobeads was a problem in this research. Each preparation of the silica had to be tested for antibody coverage. The amount of antibody bound to the silica ranged from less than 1 mg antibody/g of silica to greater than 15 mg/g depending upon the preparation.

Because of the problems associated with the membranes used in this sensor design, a sensing tip design which used a rigid opaque frit was sought as a replacement for the membrane. This required some modifications to the tip construction method and is described in the next section.

Fritted sensor

Experimental

The fiber/column bundle described for the second membrane sensor was used to test two different fritted sensing chambers. In a sensing chamber design similar to that described for the membrane sensor, commercially available chromatography frits were held in place at the end of the fiber bundle with heat-shrink tubing. In a later design, specially designed cylindrical stainless steel frits were fastened in place on the bundle using epoxy cement.

Experiments similar to those described for the membrane sensor were used to evaluate several different frit materials using the sensing chamber described for the membrane sensor. All frit materials were commercial chromatography frits obtained from Alltech Associates, Deerfield IL. Both ceramic and stainless steel frits were used in these studies.

Ceramic frits are recommended for chromatography of protein-containing solutions. Manufacturer's literature claims lower binding of protein to ceramic vs stainless steel frits. The ceramic frits quickly proved to be impractical for the sensor design. The frit diameter needed for the sensing chamber was approximately 1 mm. Ceramic frits were not available in sizes of less than 1/8 " (3.12 mm). These frits were actually smaller ceramic discs (about 1.8 mm) surrounded by a plastic or nylon sleeve. Removing the sleeve left a frit that was closer to the desired diameter, but very fragile.

The process of removing the ring frequently caused damage to the edges of the ceramic frit, making a good seal between the heat-shrink and frit impossible.

Stainless steel frits had the potential for protein adsorption problems, but were more durable and came in 1/16" (1.6 mm) diameter, making their application to the sensing chamber more practical.

Specially fabricated cylindrical stainless steel frits with 0.5 μm porosity were obtained from Newmet Krebsoge, Terryville, CT. Unlike the frits described earlier, which were drilled in-house (see page 46), this frit design seemed to be permeable in all directions. The frits, with an inside diameter of approximately 1.6 mm, were attached with epoxy so that a sensing chamber was formed with dimensions of approximately 1.6 mm diameter and 0.5 mm high, giving a volume of approximately 1 μl.

With the stainless steel frits it was important to remove all air from the frits during a conditioning procedure. This was accomplished by forcing water through all leads and out the frit for several minutes, then aspirating in solution through the frit and checking for bubbles. Air bubbles inside the capillary columns were visible with the naked eye. This procedure was repeated until no further bubbles appeared in the capillary columns during the aspiration stage. Use of a 25 % (v/v) ethanol solution for the aspiration step seemed to aid in dispelling the air trapped in the

frit. Leaks in the capillary columns or syringe valves could also be detected and corrected during this conditioning procedure.

Experiments with this sensor involved determining appropriate injection volume and slurry concentration for the immunobeads, reproducibility of immunobead and other reagent injections, reproducibility of aspiration. Procedures for these studies have been described for the membrane sensor in the previous section.

Studies were also conducted to compare the response of several different sensors to batch reacted immunobeads. These beads were prepared by incubating 1 ml of the 10 mg/ml immunobead slurry with 0.2 mg/ml FITC-IgG for several minutes, then rinsing by centrifugation; the beads were then resuspended in 1 ml of PBS buffer.

Results and discussion

The fritted sensor using the flat frits and heat-shrink tubing was quickly determined not to be a practical design. A good seal between the heat-shrink and frit was virtually impossible to achieve. Using epoxy cement to improve the seal usually caused occlusion of the pores in the frit. Tests of the few sensors deemed to be leak-free showed that rinsing out of batch beads was difficult and required a mixture of aspiration and rinsing, using large volumes of rinse solution. These problems were believed to be caused by entrapment of the beads between the edges of the frit and the heat-shrink tubing. Repeat injections of beads into the sensor eventually

led to clogging of the frit, made evident by lack of solution flow out the frit.

The remainder of this discussion will be in reference to the cylindrical frit, which seemed to offer the best potential for a useful sensor design.

As with the membrane sensor, it was found that a smaller injection of more concentrated bead slurry gave the best balance of signal, flushability, and injection time. Results of the experiment are summarized in Figure 2.16. A 50 µl injection of 10 mg/ml slurry seemed to be optimum for this sensor.

Table 2.3 summarizes the results of the experiments to determine rinsing, diffusion, and aspiration characteristics of the sensor. As can be seen from the data, diffusion did not occur into this sensor to a significant extent, but aspiration seemed to be an acceptable sampling method. This sensor seemed to allow better rinsing out of excess reagents, making it a more promising candidate for use in a real assay than the membrane sensor.

Table 2.4 summarizes the results of experiments to determine reproducibility of injections of batch immunobeads. Reproducibility of injections for this sensor design was fairly good, and sensor-to-sensor reproducibility was much better than that obtained for the membrane sensor. Signals from the batch immunobeads were much smaller for this sensor. The immunobeads used for these experiments were prepared at a different time from those used for the membrane sensor. Preparation-to-preparation reproducibility of

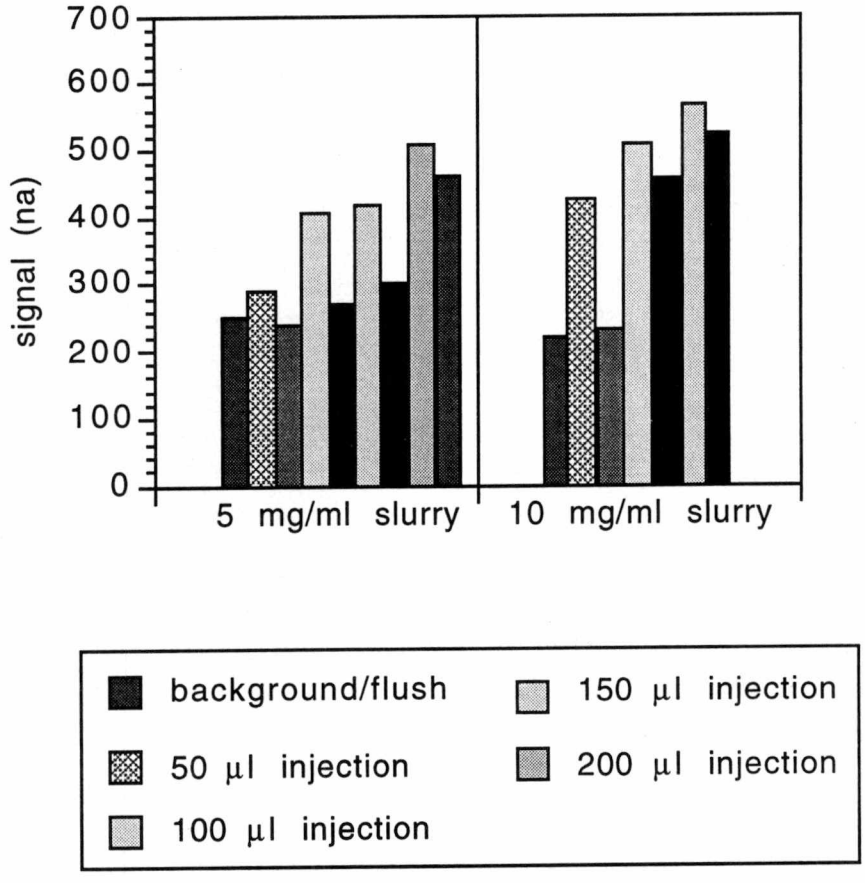

Figure 2.16. Injection of immunobeads into fritted sensor. Signal from different bead densities and injection volumes.

Table 2.3 Signal and Reproducibility data for isolated affinity steps in cylindrical frit sensor.

Measure-ment	Back-ground signal (na)	Delivery of blank beads (na)[a]	Rinse signal (na)[b]	Delivery of FITC (na)[c]	Rinse signal (na)[b]	Flush signal (na)[d]	Diffusion of FITC (na signal after 20 minutes)[e]	Diffusion of FITC-IgG (na signal after 20 min)[e]	aspiration of FITC signal(na)/ volume aspirated (µl)[e]	aspiration of FITC-IgG signal(na)/ volume aspirated (µl)[e]
1	4.0	4.8	4.8	156	5.0	4.4	8.2	6.1	88/15.0	118/14.9
2	4.1	5.5	5.4	160	5.2	4.0	7.1	5.3	85/14.6	125/15.3
3	4.2	5.2	5.2	165	4.8	4.3	6.3	6.3	87/14.9	128/15.2
4	4.1	4.6	4.7	155	5.1	4.5	7.8	6.8	83/14.2	116/14.8
5	4.0	4.4	4.3	153	4.8	3.8	8.0	5.0	91/15.3	118/14.7
average	4.1	4.9	4.9	158	5.0	4.2	7.5	5.9	87/14.8	121/15.0
CV	2.1	9.1	8.8	3.0	3.6	6.9	10.4	12.5	3.5/2.8	4.3/1.7

Notes: See experimental section for more detail

a. 50 µl of 10 mg/ml, 10 µm diameter blank silica beads

b. 100 µl of water delivered to sensing chamber via rinse inlet leads

c. 50 µl of 10^{-4} M FITC delivered to sensing chamber with blank beads in place

d. Sensor flushed out with water to remove beads and remaining FITC

e. FITC concentration = 10^{-4} M, FITC-IgG concentration = 0.5 mg/ml. Volume measured by expulsion of aspirated sample and dilution to 1ml. Absorbance of this solution was measured and compared to a calibration curve derived using fixed volume of "sample" solutions diluted to 1ml

Table 2.4 Reproducibility of immunobead injections for three different cylindrical frit sensors.

Measurement	Sensor #1		Sensor #2		Sensor #3	
	inject (na)[a]	flush (na)[b]	inject (na)[a]	flush (na)[b]	inject (na)[a]	flush (na)[b]
1	68	8.5	78	9.1	71	6.8
2	75	9.2	82	9.8	75	7.2
3	71	8.3	91	8.7	70	7.0
4	82	8.8	89	8.8	82	6.9
5	76	8.5	86	9.0	76	7.4
average	74	8.7	85	9.1	75	7.1
CV	7.2	4.0	6.2	4.8	6.4	3.4

Notes:

a. 50 µl of 10 mg/ml immunobeads, batch reacted with FITC-IgG. Injection accomplished using 50 µl injection loop followed by approximately 200 µl of rinse solution.

b. Sensor flushed out with water until stable signal attained, usually about 0.5 ml of rinse solution required

immunobead labeling was extremely poor, so all experiments with a single sensor had to be performed using immunobeads prepared at the same time. The smaller signals may have also been due to a smaller sensor volume

The cylindrical frits were durable, but had a tendency to become clogged after several hours of use. This may have been due to adsorption of protein onto the stainless steel frit material, or due to deterioration of the epoxy cement used to construct the sensing tip. Removing the frit and "baking" it in a furnace at approximately 400^{o}C for 10-15 minutes, followed by ultrasonic cleaning in 1 M HNO_3 for several minutes, helped to clean the frit for use on another sensing tip. This allowed several reuses of a frit before it became irreparably clogged. The process of removing the frit damaged the sensor tip to such an extent that it could not be reused. These problems with the frit and sensor design led to a search for other materials for use in construction of the sensor and for a tip design that allowed use of other frit materials.

The experiments described in this chapter revealed several important considerations in the design of fiber optics based immunochemical sensors. These include the necessity of optimizing the concentration of immobilized antibody, the benefits of an active sampling and reagent delivery system, and the importance of standardized construction methods with replaceable parts. The experiments also revealed several areas that would benefit from further refinement. The mechanical aspects of the reagent delivery

system seemed to function well, although air leaks were a frequent frustration and the column sealing method was somewhat awkward. The relatively short useful lifetime of the fritted sensors, and the need to reevaluate each new sensing tip, suggested that further modification of the sensor construction procedure was needed. Reproducibility of antibody and analyte coupling to the immunobeads also needed improvement. These issues are addressed in the next chapter which describes a redesigned sensor and comprehensive studies of the immunobead preparation procedure.

CHAPTER 3

DEVELOPMENT OF A SANDWICH FLUOROIMMUNOASSAY FOR THE DETECTION OF IgG USING A REGENERABLE FIBER OPTIC SENSOR

Introduction

The experiments described in Chapter 2 revealed that, of the approaches tried, the best approach to the design of a true sensor (as opposed to a probe) seems to be that of a regenerable sensor---one in which the reagents can be replaced *in situ*. Another possible approach, which was not tried, was the equilibrium competitive binding approach.

The fritted sensor described in the last chapter allowed regeneration of reagents, but the sensor itself functioned only marginally well as a detection device. Deterioration of the performance of the sensor with time was the largest problem, followed by lack of reproducibility in construction and in immunobead preparation.

These problems were addressed with a new construction method for the sensor that employed a water resistant resin and allowed for testing of different frit materials. Research into different antibody immobilization procedures gave valuable insight into the limitations of immunoassay techniques. The new sensor

design and the results of the immobilization research will be presented in this chapter, along with the results of direct and sandwich immunoassays for IgG using the sensor.

Immobilization of Antibody.

In the experiments described in Chapter 2, an antibody immobilization procedure was used in which GOPS derivatization of the glass was followed by periodate activation and covalent coupling of antibody to the glass. This method led to wide variations in the amount of antibody coupled to the glass, due in part to the nature of the surface being treated, but large variations also occurred between different preparations on the same type of surface.

Control of the amount of antibody bound to the surface of the immunobeads and standardization of the immunoreactivity is desirable for immunosensor design. Large quantities of immunobeads are needed for characterization of new sensors. If the amount of antibody bound to the beads varies each time they are prepared calibration of the sensor will become quite difficult, if not impossible, since all trials will have to come from the same preparation of immunobeads. In addition, if coverage of antibody on the immunobeads is not reproducible, each new preparation of beads will need to be calibrated in a working sensor. A technique for immunobead preparation that allows either large preparations or reproducibility from one preparation to the next is necessary to

provide immunobeads in the quantities needed for sensor design and ultimately for practical use of the sensor.

Because of the cost of materials and uncertainty regarding long-term storage of immunobeads, it was determined that reproducibility of immunobead preparation rather than large-scale production was a more practical approach.

A literature review of other immobilization techniques (89-92) indicated that an immobilization method using carbonyldiimidazole (CDI) to activate GOPS derivatized silica might be more reproducible and preserve more antibody activity. Several variations of this method were tested in an attempt to find that which best suited the intended application.

The experiments using the membrane sensor and fritted sensor indicated that spherical silica has the best flushing characteristics for this type of sensor. All experiments described in this chapter used spherical silica, but the pore size and particle size were varied.

Experimental

The procedure for preparation of diol silica by GOPS derivatization of silica spheres was essentially the same as described in Chapter 2. The silica was rinsed with hot nitric acid, sonicated for 15 minutes to remove air bubbles, then rinsed with 100 ml of distilled water. The silica was then suspended in 20 ml of 10%(v/v) aqueous GOPS (Aldrich Chemical Company, St Louis, MO)

solution with the pH adjusted to approximately 3. The GOPS-silica mixture was heated, with stirring, at 90°C for 3 hours. During this process the volume was replenished with water and 1M HCl was used to keep the pH at 3. It was found that allowing too much water to evaporate, or the pH to vary too widely, caused the GOPS to polymerize into a sticky goo, ruining the silica, and quite frequently the container.

The silica was filtered and rinsed and dried overnight. Two different methods were used for the drying. In the first the silica was dried at 110° C under atmospheric pressure. The other method involved drying in a vacuum oven at 110°C--this method was supposed to remove all moisture from the pores of the silica.

Activation of the diol silica with carbonyldiimidazole (CDI) was as follows. 320 mg of 1,1'- carbonyldiimidazole (Sigma Chemical Company, St Louis MO) was dissolved in 2 ml of acetonitrile and 20-100 mg of diol silica was suspended in the solution. The mixture was degassed ultrasonically for 15 minutes, then shaken at room temperature for 30 minutes. The beads were filtered and rinsed with 50 ml of acetonitrile to remove any remaining CDI. The acetonitrile was allowed to evaporate and the dried beads were rinsed with several 10 ml aliquots of phosphate buffered saline (PBS). The PBS was removed by filtration, but the beads were not allowed to dry. The final PBS solution was removed by centrifugation. The activated silica was incubated, with stirring,

in the appropriate amount of anti-IgG solution at 4 ^{o}C for up to one week.

Binding of antibody to the silica was measured as described in Chapter 2 (page 29) by monitoring the decrease in absorbance at 280 nm of the antibody solution. FITC-labelled IgG solutions were used to verify retention of antibody activity with immobilization. The absorbance of these solutions was measured at both 280 and 488 nm. Several different concentrations of analyte were incubated for varied times at room temperature to monitor the antibody activity.

Results are reported for the following silica spheres: 5 μm and 10 μm diameter Spherisorb silica (80 Å pore size) and 10 μm Nucleosil (500 Å pore size) both purchased from Alltech Associates, Deerfield, IL)

Results and Discussion

Preparation of the immunobeads in an economical fashion required optimization of incubation times and initial concentration of antibody. The results of this study are reported in Table 3.1. The data indicate that increasing concentration of antibody or incubation time does not necessarily increase the amount of antibody bound to the silica. This suggests that the main controlling factor of antibody binding to the silica may be the total number of active sites available for binding. This is controlled by several factors, including the number of diol groups following the initial derivatization process with GOPS, the effectiveness of the CDI activation, the

Table 3.1. Binding of anti-IgG to CDI derivatized silica. Comparison of amount of antibody bound with incubation time and initial concentration of antibody.

Initial antibody concentration	Amount of antibody bound (mg anti-IgG/g silica)* 12 hour incubation	24 hour incubation	48 hour incubation
0.10 mg/ml	4.25	7.48	7.97
0.15 mg/ml	6.35	8.55	9.45
0.20 mg/ml	5.50	7.50	8.20

* Silica used was 10 μm diameter Spherisorb (80 Å pore size). Data reported are average for 3 identically prepared samples. All samples came from the same batch of derivatized silica.

surface area of the silica, and the speed with which the active sites are hydrolyzed and made inactive by contact with aqueous buffer.

Crowley and coworkers (92) reported that complete hydrolysis of CDI binding sites can take as much as 6 days in phosphate buffer. This paper studied extensively the effects of GOPS coverage, concentration of CDI, choice of buffer, surface area of the silica and concentration of antibody on the binding of anti-human IgG to silica. Their results suggest that increasing concentration of antibody should increase the coverage on the silica, and they were able to achieve coverages as high as 100 mg Ab/g of silica for silica with 500 Å pore size and 50 m^2/g surface area. The Spherisorb silica used for most of the experiments reported here had a surface area of 220 m^2/g and a pore size of 80 Å. Using Nucleosil silica with 500 Å pore size and 35 m^2/g surface area did not increase the amount of antibody bound.

One important conclusion of Crowley's research was that the concentration of CDI used must be determined empirically, but a minimum of 10 mol of CDI/ mol of diol gave the best binding in their research. Sportsman and Wilson used quantitative periodate oxidation to determine the diol coverage on GOPS derivatized glass spheres. They found 340 μequiv of diol/g of glass (91). The diol coverage of the silica used in the experiments described above was not determined experimentally; instead the concentration of CDI was estimated based on Crowley's results for silica with a smaller surface area.

Table 3.2 compares binding of the antibody to three different sizes and types of silica. It also compares the effect of drying the silica in vacuum oven versus drying at atmospheric pressure before the CDI derivatization. The results indicate that drying under vacuum significantly affects the amount of antibody ultimately bound. This is probably due to the removal of additional water exposing a greater number of diol groups on the silica. Because the 5 and 10 μm spherisorb had the same surface area one would expect the coverage of antibody on the two surfaces to be similar. The variation shown by these data could have been caused by variation in the diol derivatization or CDI activation process from one preparation to another.

This type of variation continued to be a problem throughout the research. Reproducibility of antibody binding for several preparations of immunobeads prepared from the same batch of diol silica, even for those started on different days from diol silica that had been stored in a desiccator was very good (CV < 8 %), Reproducibility for immunobeads prepared from different preparations of diol silica was much worse, frequently with a CV of more than 20 %. These data suggest that it is possible to prepare large quantities of diol silica and store it for extended periods. Immunobeads prepared at different times from the same batch of diol silica show fairly reproducible binding of antibody. It is advisable however to verify the binding of each preparation of immunobeads using UV-Vis spectrometry. This allows one to set a

Table 3.2: Reproducibility of antibody binding to CDI-derivatized silica. Comparison of drying method, size of silica spheres, and pore size of silica.

a) 5 μm Spherisorb (80 Å pore size)

	Antibody binding--mg Ab/g silica	
Sample #	air dry--110°C	vacuum dry --110°C
1	5.29	6.25
2	5.66	6.84
3	5.23	7.10
4	5.08	6.52
5	5.63	6.93
6	6.28	NA
average	5.53	6.73
CV	7.8 %	5.0 %

b) 10 μm Spherisorb (80 Å pore size)

	Antibody binding--mg Ab/g silica	
Sample #	air dry--110°C	vacuum dry --110°C
1	10.23	11.54
2	9.49	12.12
3	9.98	11.98
4	10.04	11.85
5	10.15	11.79
average	9.98	11.85
CV	2.9 %	1.9 %

c) 10 μm Nucleosil (500 Å pore size)

	Antibody binding--mg Ab/g silica
Sample #	vacuum dry --110°C
1	8.55
2	8.48
3	8.96
4	8.41
5	8.50
average	8.58
CV	2.5 %

"target" range of acceptable antibody coverage and to discard any outlying samples. This method is not as successful as was hoped, since there is still the risk of loss of an entire preparation of beads due to unacceptable binding. If one desired to immobilize monoclonal antibodies, available only in very small quantities, this method might quickly become prohibitively expensive.

Table 3.3 illustrates the retention of antibody activity by the immunobeads. Two different preparations of immunobeads were used to determine if analyte binding increases with increased antibody concentration. These results seem to indicate that there is an optimum antibody concentration on the silica above which there is only a slight increase in the amount of analyte bound. These results also indicate that binding of analyte occurs fairly rapidly for these immunobeads, an important consideration in a sensor in which the analyte containing sample flows past the immunobeads.

Construction and Characterization of the Sensor

The experiments described in Chapter 2 revealed the strengths of a reagent delivery approach to regenerable sensing, but the sensor function as a detection device left something to be desired. Irreproducibility in construction of sensors was believed to be a probable cause as was the limited choice of frit materials and the use of epoxy resins that seemed to deteriorate with long term exposure to aqueous solutions.

Table 3.3: Binding of FITC-labeled IgG to Immunobeads. Comparison of concentration of FITC-IgG, incubation time, and amount of antibody bound to 10 μm diameter Spherisorb silica.

a. 9.6 mg Ab/g silica Immunobeads, 10 mg/ml bead solution density

IgG concentration (mg/ml)	Amount of IgG bound (mg IgG/g silica) 2 min	5 min	10 min
0.10	4.8	5.6	5.9
0.05	3.4	3.8	4.4
0.025	1.2	1.8	2.1

b. 5.4 mg Ab/g silica Immunobeads, 10 mg/ml bead solution density

IgG concentration (mg/ml)	Amount of IgG bound (mg IgG/g silica) 2 min	5 min	10 min
0.10	3.4	4.5	4.9
0.05	2.8	3.6	4.2
0.025	1.2	1.8	2.2

A new method of sensor construction was devised that allowed casting of the sensor components using an acrylic resin. The resin was much more water resistant than the epoxy used in earlier designs, and the design of the sensing chamber was modified so that a variety of frit materials could be tested for durability and permeability.

Experimental

Note: Portions of the following research on sensor design and construction were done in cooperation with James R. Bowyer and have also been reported elsewhere (78, 88). All data reported are original to this dissertation.

The sensor body and sensing chamber were molded using an acrylic casting resin (Castin' Craft Clear Liquid Plastic Casting Resin, ETI, Fields Landing, CA---purchased locally at Michael's Arts and Crafts). The molds for the casting process were prepared in-house. Frit materials were purchased from Alltech Associates, Deerfield IL. and from Baxter Scientific Products. Optical fibers were purchased from General Fiber Optics, Cedar Grove NJ. Capillary columns were purchased from Polymicro Technologies, Phoenix AZ.

The acrylic resin is a two component system that is mixed in a manner similar to epoxy, but which takes two hours to reach a gelatinous state and hardens completely in about 6-8 hours. This characteristic makes it amenable to an injection molding technique.

Once hardened the resin is much more impervious than epoxy to water and some organic solvents. The molds used for construction of the sensing tip and chamber are illustrated in Figures 3.1 and 3.2.

Construction of the sensing tip was accomplished as follows. Short lengths (5-8 cm) of 200 μm id capillary column were inserted into the small holes in the mold and template. To allow for easier identification of opposing columns once the tip was cast, columns that were opposite to each other were cut to the same length. A 400 μm fiber optic with approximately 1 cm of cladding removed was inserted in the center hole of the mold and template. To allow for easier removal of the tip after casting, the mold was coated with a thin layer of vacuum grease before the tubing and fiber were inserted. It was important that 1-2 mm of column be left outside the mold on the closed end so that the columns were not occluded with resin during the casting process. The mold and template were then taped to a desk-top to prevent movement during the casting process. Resin was added to the mold using a 27 gauge needle and 5 cc syringe. The mold was overfilled slightly to aid in removal of air bubbles. Once the resin was hardened the mold could be removed by warming gently with a flame and pulling very gently on the columns and fiber. The sensing tip was then polished and appropriate reagent delivery and rinse leads were connected to the 200 μm columns. This assembly was essentially the same as that described in Chapter 2. Two 200 μm columns led to the aspiration "T" which had two 520 μm columns for use in aspiration and delivery of sample and rinse

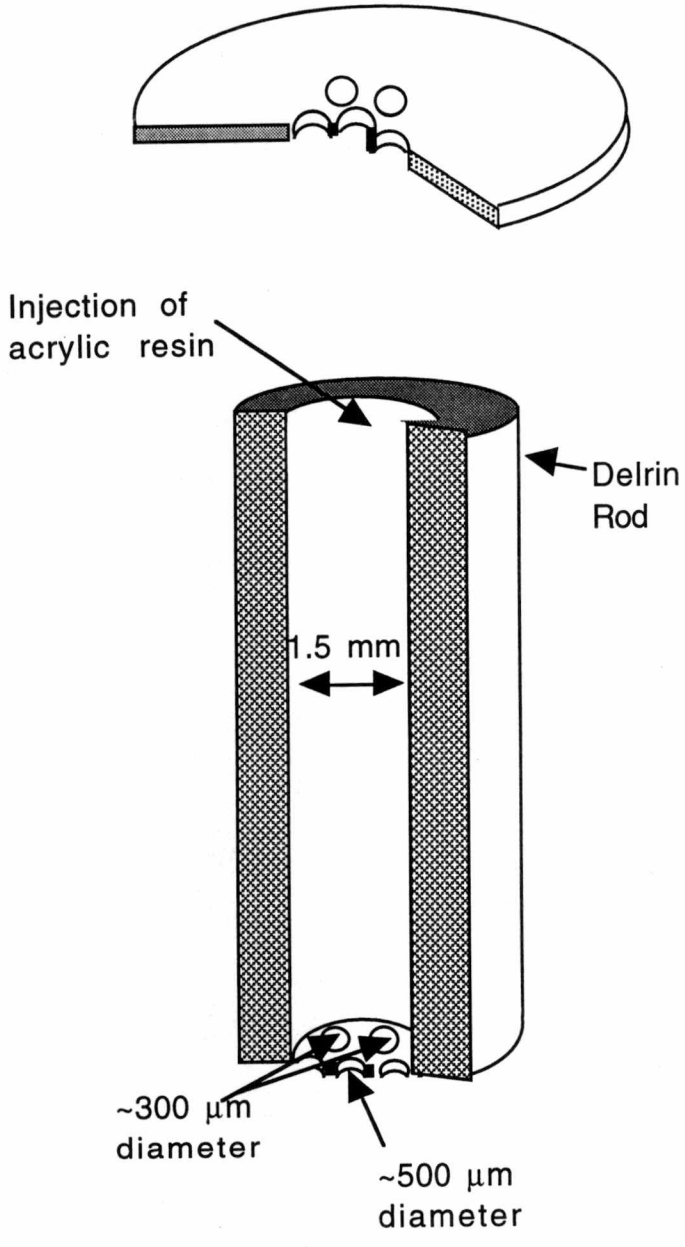

Figure 3.1. Sensing tip mold and template.

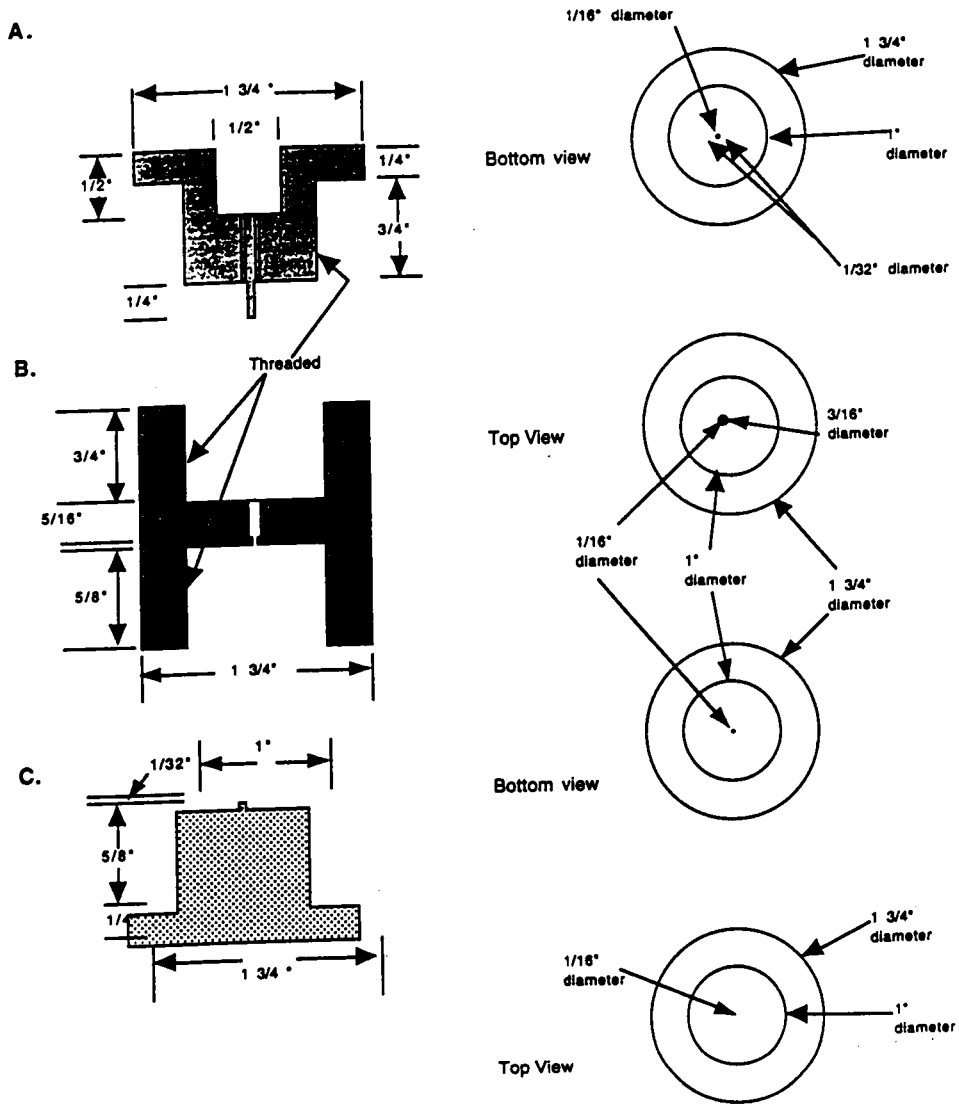

Figure 3.2. Sensing Chamber Mold components. A) Top plug B) Center compartment C) Bottom Plug.

solutions. A 320 μm column attached to an injection loop served as the bead delivery column, and another 320 μm column was used to deliver rinse solutions. Two 520 μm columns served as outlets during the flushing process.

The sensing chamber mold was designed to hold the frit material. Some of the frit materials required preparation before being placed in the mold. Thin porous Teflon frits were prepared from sheets of porous Teflon (2 μm porosity) by making thin slices with a very sharp razor blade. The goal was to prepare frits with a fairly uniform thickness of less than 1 mm with dimensions of 5 mm square, a goal that was attained only with great patience and many miscuts. For the other frit materials trimming to fit the mold was the only preparation necessary.

Figure 3.2 illustrates the mold assembly. The upper plug forms the interior of the sensing chamber into which the tip will be inserted. The lower plug serves to hold the frit material in place. There were two different configurations of this plug to allow use of different frit materials. When the two plugs were screwed into the mold body they sandwiched the frit material between them, hopefully tightly enough to prevent occlusion of the frit by casting resin, but gently enough to avoid damaging the pores in the softer frit materials. When the resin hardened, the exposed edges of the frit were enclosed in resin, holding the frit in place at the end of the sensing chamber. The two versions of the lower plug allowed for use of different frit materials. The shorter plug leaves a recessed area

at the end of the mold. This was used to hold 1/16" stainless steel frits (1/32" thick). The longer plug actually creates a slightly raised "platform" inside the mold. Thinner, softer frit materials were placed here and the resin partially covers the bottom of the frit material, adding stability.

This mold was also coated with a thin layer of vacuum grease to aid in removal of cast parts after the resin hardened. Resin was added to the mold via the holes in the upper plug. One hole was for introduction of the resin, the other allowed air and excess resin to escape. After the resin hardened the plugs were removed and fritted chamber was removed from the upper plug by applying gentle heat and a slight twisting motion. Excessive heat will damage the frit material and too much force will damage the mold or crack the resin.

The sensing tip and sensing chamber were assembled using epoxy cement to secure the chamber to the tip. Because the chamber was transparent it was possible to measure the exact distance between the sensing tip and the frit. Generally a distance of 0.5 mm was used, giving an approximate sensor volume of 1μL. Once assembled the apparatus was connected to a syringe pump with all but the inlet lead closed and tested for leaks. As one might expect, the epoxy connections were the most common leak points, either around the resin tip, or where the leads were spliced into the tip.

Once the sensor was determined to be leak free, several experiments were performed to characterize the sensor response. The detection apparatus was similar to that described in Chapter 2

with two exceptions. The laser used in these experiments was a HeNe "greenie" laser operating at 543.5 nm (PMS Electro-optics, Boulder, CO). Instead of a dichroic filter a mirror with a hole in the center (prepared in-house) was used to separate the incident light from the fluorescent signal. Using the green line laser required changing the fluorescent dye from a fluorescein based dye to a rhodamine dye.

These experiments included determining appropriate injection volume and slurry concentration for the immunobeads, reproducibility of immunobead and other reagent injections, reproducibility of aspiration. The procedure for these experiments, changed little from that described in Chapter 2, is outlined briefly here.

Preliminary tests were performed to determine flow characteristics of the sensing chamber before the addition of bead slurry. These tests used dilute tetramethyl rhodamine B isothiocyanate (TRITC) solutions to determine the maximum flow rate possible for reagent delivery with each membrane. Immunobeads (antibody bound to silica) were prepared in the manner described above. Some of the immunobeads were pre-reacted with TRITC-IgG to create a fluorescent signal that would allow monitoring of the beads as they were injected into the sensor tip. These beads were prepared by centrifuging 1 ml of 10 mg/ml bead slurry and removing the supernatent, then incubating the remaining silica with 1 ml of 0.10 mg/ml TRITC-IgG for 30 minutes. The

solution was then centrifuged, the unreacted TRITC-IgG removed and the silica resuspended in 1 ml of PBS buffer. Pre-reacted bead slurry was injected into the sensor using an injection loop to control the volume. Repeat injections without flushing of the sensor helped to determine the optimum injection volume. Conditions were sought that gave a large signal but also allowed complete flushing of the beads from the sensor in a reasonable time.

Once an optimum bead concentration and injection volume were chosen, reproducibility of slurry injection was studied with repetitive injections of the pre-reacted immunobeads.

To examine the rinsing characteristics of the sensor, a 50 μl injection of blank silica (10 mg/ml) was followed by a 50 μl injection of TRITC through the same lead. A rinse solution of PBS buffer was then delivered using the syringe pump to control flow rate. The time required for return to a baseline was used to measure the volume of rinse required.

Sampling by aspiration was studied. As with the sensors described in Chapter 2, a "T" design attached to the aspiration column allowed control of the amount of sample delivered. This "T" was illustrated in Figure 2.14. Reproducibility of aspiration was studied with TRITC-labeled IgG. Instead of expelling the aspirated "sample" from the sensor, as described in Chapter 2, the signal upon delivery of aspirated sample to the sensing chamber was used as an indication of reproducibility of aspiration.

Results and Discussion

Several different frit materials were tested in the sensing chamber. Stainless steel chromatography frits (2 μm pore size, 1/16 inch diameter, Alltech Associates) had a tendency to leak around the edges when solution flow rate exceeded 5 μl/min. In addition the surfaces of these frits appeared to be quite rough allowing immunobeads to collect on the surface and clog the frit. The acrylic resin did not seem to adhere well to the stainless steel; the frits could be popped out of the sensing chamber with solution flow rates of about 20 μl/min.

Porous membranes (5 μm polyester, polycarbonate, and cellulose ester) presented similar problems to those discussed in Chapter 2. When pressure was applied, these materials bowed out and stretched until they failed. Ceramic frit material is recommended for protein applications, but the standard sizes of ceramic frits were too large for the sensing chamber. Attempts to trim them to size were largely unsuccessful; the frit material was very fragile and shattered readily. The Teflon frit material worked well for this application. The thickness of the frit could be varied to control the tendency to bow or stretch under pressure. The Teflon frit material with a 2 μm porosity cut to approximately 1 mm thick could withstand flow rates of as much as 40 μl/min when the sensing chamber was empty. When beads were injected into the sensor it was generally necessary to reduce the flow rate to approximately 15 μl/min to prevent backpressure buildup causing

the syringe pump to slip. The Teflon frits did not blow out even under conditions that caused the pump to slip.

The results reported in Figure 3.3 indicated that the optimum injection volume for this sensor was a single 50 µl injection of 10 mg/ml bead slurry. Larger injections gave greater signals, indicating that the sensor was not filled with a single injection, but flushing of the sensor became more difficult with each successive injection. Repetitive 50 µl injections of the immunobeads used for the injection volume study gave an average signal of 42.4 na with a CV of 4.6 % for 10 injections.

Figure 3.4 illustrates the rinsing characteristics of the sensor. At a rinse flow rate of approximately 14 µl/min it took approximately 10 minutes to return to a stable signal. This corresponds to 140 µl of rinse solution. This signal was slightly higher than the background for the empty sensor and the signal from the sensor containing only blank silica, indicating that some of the TRITC was being retained by the beads. The sensor used for this experiment could not tolerate a higher flow rate without the pump slipping; other sensors could tolerate a slightly faster flow rate, decreasing slightly the time required for rinsing.

Table 3.4 summarizes the results of aspiration studies with the sensor. The signal during aspiration was generally higher and somewhat noisier looking, but was fairly reproducible. The signals during sample delivery were less noisy and had symmetric shape. These signals were less noisy than the background signals following

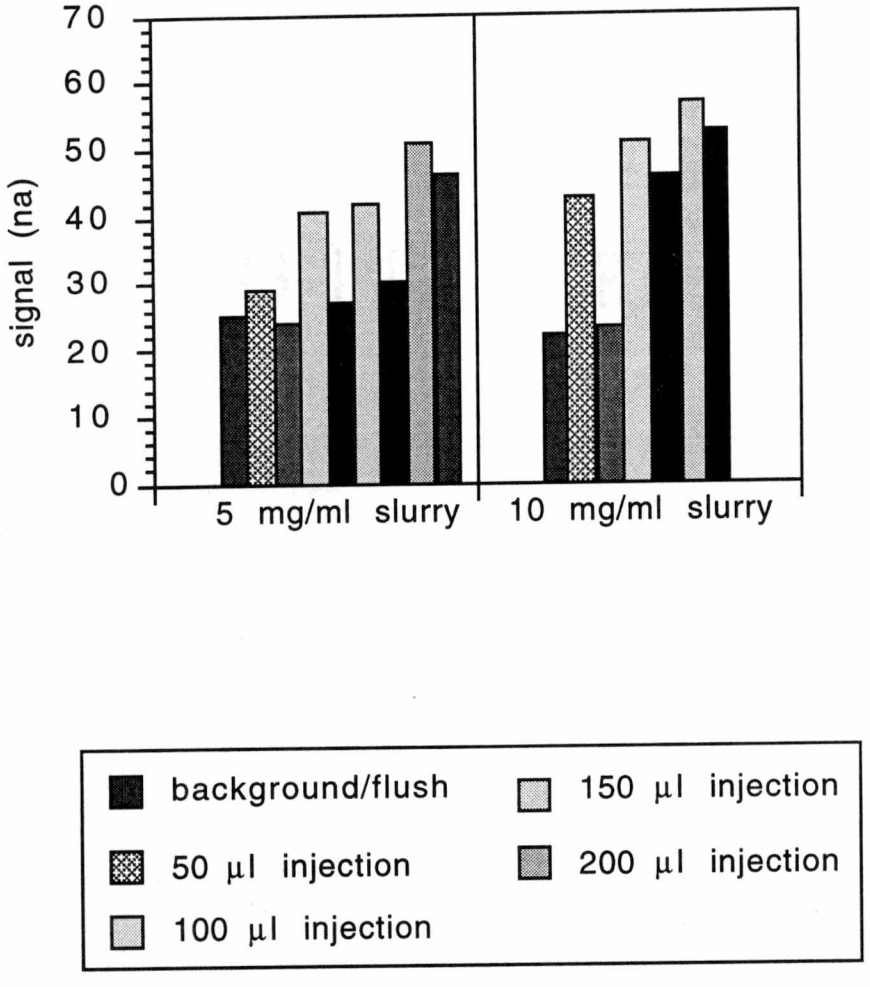

Figure 3.3. Injection of immunobeads into acrylic sensor. Signal from different bead densities and injection volumes.

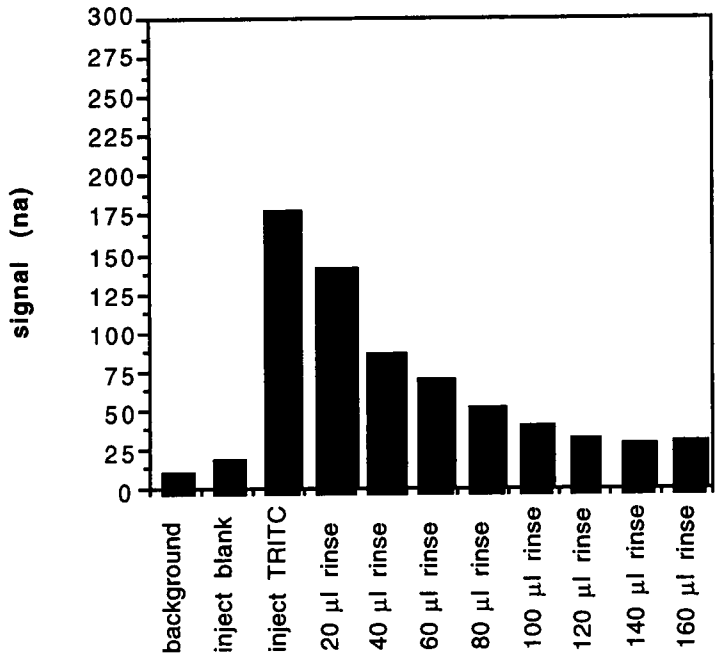

Figure 3.4. Rinsing characteristics of acrylic sensor with teflon frit.

Table 3.4. Reproducibility of Aspiration of TRITC labeled IgG (0.10 mg/ml) into acrylic sensor with Teflon frit.

a) 20 µl aspiration

	background signal (na)	peak signal (aspiration) (µa)	peak signal (sample delivery) (na)	background signal (na)
Sample 1	12.1	1.54	956	15.2
Sample 2	15.2	1.49	932	13.7
Sample 3	13.7	1.52	975	16.5
Sample 4	16.5	1.68	981	18.1
Sample 5	18.1	1.42	924	21.0
average	15.1	1.53	954	16.9
CV	16 %	6.2 %	2.6 %	16 %

b) 40 µl aspiration

	background signal (na)	peak signal (aspiration) (µa)	peak signal (sample delivery) (na)	background signal (na)
Sample 1	15.6	1.59	985	17.2
Sample 2	17.2	1.46	926	15.8
Sample 3	15.8	1.62	948	18.0
Sample 4	18.0	1.70	958	21.1
Sample 5	21.1	1.48	954	24.0
average	17.5	1.57	954	19.2
CV	13 %	6.3 %	2.2 %	17 %

rinsing. The background signals during this study rose slightly with repeat samples, indicating a memory effect which was not noticeable in the much higher signals from the fluorescently labeled samples. In each case the background reported was stable, just slightly higher than the previous background signal.

The data collected in these experiments indicated that, although construction of new sensors was not completely reproducible, the background signals and signals from TRITC solutions were reproducible for each sensor. This suggests that it might be possible to standardize signals from different sensors using experiments such as those described above.

Analysis of IgG

Once characterized and determined to be working properly, the sensor was used for the analysis of IgG in solution using both a direct assay and a sandwich assay. IgG was chosen as a representative protein molecule for these assays due to its ready availability with a number of different fluorescent tags. IgG itself is becoming a more important analyte molecule as researchers have discovered four different subclasses of human IgG. These subclasses have been linked to several autoimmune disorders and immunodeficiency syndromes in human patients (83, 84).

Direct Assay

The direct assay is generally used for an analysis where the analyte is itself naturally fluorescent. Very few large analytes are naturally fluorescent to the extent that fluorescence could be used as a detection technique, so these experiments with TRITC-labelled IgG as the analyte were used as precursors to analysis by a sandwich assay. These experiments allowed separation of the sandwich assay into component steps to allow optimization of the sensor for each step. These steps are outlined in Table 3.5

Experimental

Rabbit IgG , anti-rabbit IgG, TRITC-labelled rabbit IgG, and TRITC-labeled anti-rabbit IgG were obtained from Sigma Chemical Co. In the direct assay, solutions of TRITC-labeled IgG were studied (TRITC-IgG). In the sandwich assay unlabeled IgG was the analyte (IgG) and the TRITC-labeled anti IgG (TRITC-Ab2) was used as an indicator antibody. Unless indicated otherwise, all solutions were prepared in pH 7.4 phosphate buffered saline solution, prepared in house and preserved with sodium azide. The general principles of both direct and sandwich immunoassays were discussed in Chapter 1.

The apparatus described above was used for the direct assay. In order to determine if immunobeads reacted with TRITC-IgG would be visible with the sensor configuration described above, beads containing both anti-IgG (Ab1) and TRITC-IgG were injected into the

Table 3.5 Protocol and related design factors for sensor-based sandwich immunoassay .

1. Aspirate sample into holding column--must be able to aspirate a reproducible quantity.

2. Deliver immunobeads to sensor--quantity of immunobeads delivered must be reproducible, antibody coverage on immunobeads should be reproducible.

3. Deliver sample to immunobeads--flow rate of delivery may affect binding of analyte to antibody.

4. Rinse unbound analyte from sensor--flow rate may affect ability to rinse completely.

5. Deliver second antibody--concentration of antibody and flow rate must be optimized.

6. Rinse unbound antibody from sensor--flow rate should be optimized.

7. Measure fluorescent signal.

8. Flush sensor--for repetitive operation, sensor should rapidly return to a stable background signal, preferably the same background as at the start of the experiment.

sensor. Results are reported for injection of beads prepared from the same concentration of TRITC-IgG in three different sensors and for beads prepared with different concentrations of TRITC-IgG solution injected into a single sensor. It was important to control the reaction conditions when preparing these beads so that any observed differences in signal came from concentration of analyte, not reaction conditions.

Once it was determined that the sensor could "see" different concentrations of batch beads it was used in a method more like the purpose for which it was designed. Immunobeads were injected into the sensor tip and TRITC-IgG was flowed past the beads. Rather than introducing any sampling error at this stage, the TRITC-IgG was delivered through the same injection loop as that used for bead introduction, and the delivery rate was varied to determine the effect of flow rate on sensor signal. Once an optimum flow rate was chosen, aspiration of sample was added to the process. Sample aspiration was accomplished as described above. Four different TRITC-IgG concentrations were aspirated as well as an unknown "sample" of TRITC-IgG in phosphate buffered saline (PBS). A calibration curve was constructed from the data for the standards. The concentration of the unknown was verified by UV-VIS spectrometry. A calibration curve was also prepared for TRITC-IgG in a PBS solution that also contained 0.05 mg/ml ovalbumin and 0.05 mg/ml goat IgG (Sigma Chemical Co, St Louis, MO) to represent a more complex sample matrix.

Results and Discussion

Table 3.6 illustrates the injection of the batch beads into three different sensors. As indicated by the large variation in both background signal and the bead signal from sensor-to-sensor, reproducibility in sensor construction was still a problem. There were several factors involved in the sensor design that might have caused this. One was the polishing of the distal surface of the fiber. The surface of each fiber was examined under a dissecting microscope before the sensor was constructed for evidence of scratches or other surface irregularities. Each was deemed to be polished to a mirror smooth surface, but it was impossible to judge if the surfaces were identical. The thickness of resin next to the fibers and the exact positioning of the columns around the fiber varied from sensor to sensor despite the use of the molds. This might affect the properties of any reflected light as well as any evanescent radiation.

Another variation might have come from the positioning of the sensing tip inside of the sensing chamber. This step required measurement of the distance from the end of the sensing tip to the frit. All were constructed so that the distance was approximately 0.5 mm, but occasionally this distance changed as the epoxy resin hardened. Any change in the volume of the sensing chamber might cause a change in the measured signal from the beads in the chamber.

Table 3.6 Reproducibility of immunobead injections for three different acrylic sensors with Teflon frits.

Measurement	Sensor #1		Sensor #2		Sensor #3	
	inject (na)[a]	flush (na)[b]	inject (na)[a]	flush (na)[b]	inject (na)[a]	flush (na)[b]
1	35	5	48	11	85	24
2	42	4	51	10	81	21
3	32	5	46	11	84	22
4	38	6	49	12	86	23
5	41	6	51	11	85	21
average	38	5	49	11	84	22
CV	11 %	16 %	4.3 %	6.4 %	2.3 %	5.8 %

Notes:

a. 50 µl of 10 mg/ml immunobeads, batch reacted with TRITC-IgG. Batch prepared by reacting 1 ml of 0.1 mg/ml TRITC-IgG with 10 mg of immunobeads. Injection accomplished using 50 µl injection loop followed by approximately 200 µl of rinse solution.

b. Sensor flushed out with water until stable signal attained, usually about 0.5 ml of rinse solution required

Another difficulty was in alignment of the fiber into the apparatus. Each new sensor required some realignment of the laser beam to compensate for differences in the placement of the fiber into the holder. Each fiber was aligned before the sensing chamber was attached by optimizing the signal from 10^{-6} M TRITC solution. This signal was not the same for every sensor, indicating that some differences in the surface or alignment were unavoidable.

The data reported in Table 3.7 show that the sensor could distinguish between four different concentrations of batch immunobeads. The averages of these data were also subjected to linear regression analysis as for a calibration curve. This analysis gave a correlation coefficient of 0.997 for the straight line.

Figure 3.5 shows the effect of the rate of delivery of TRITC-IgG on the signal obtained from the immunobeads. The flow rates were determined by the syringe pump using different sizes of syringes allows more variation in the flow rate, but all data in this report were obtained using a 5 cc disposable syringe. The maximum flow rate was the setting just before that at which the pump slipped. These data indicate that at flow rates this low (136 µl/min max) there was little difference between the signals. Since the time required to deliver the 50 µl of TRITC-IgG and 250 µl of rinse was approximately 10 times longer at the lowest flow rate than the fastest, it was decided to pursue further experiments using the fastest flow rate the sensor could withstand.

Table 3.7. Comparison of four different concentrations of batch immunobeads in acrylic sensor.

Measurement	0.10 mg/ml TRITC-IgG		0.075 mg/ml TRITC-IgG		0.050 mg/ml TRITC-IgG		0.025 mg/ml TRITC-IgG	
	inject (na)[a]	flush (na)[b]	inject (na)[a]	flush (na)[b]	inject (na)[a]	flush (na)[b]	inject (na)[a]	flush (na)[b]
1	85	24	75	21	60	23	51	24
2	81	21	73	24	62	21	53	22
3	84	22	74	23	61	20	52	26
4	86	23	70	21	63	23	53	21
5	80	21	76	22	59	24	51	24
average	83	22	74	22	61	22	52	23
CV	3.1 %	5.9 %	3.1 %	5.9 %	2.3 %	7.5 %	1.9 %	8.4 %

Notes:

a. 50 µl of 10 mg/ml immunobeads, batch reacted with TRITC-IgG. Batch prepared by reacting 1 ml of TRITC-IgG solution with 10 mg of immunobeads. Injection accomplished using 50 µl injection loop followed by approximately 200 µl of rinse solution.

b. Sensor flushed out with water until stable signal attained, usually about 0.5 ml of rinse solution required

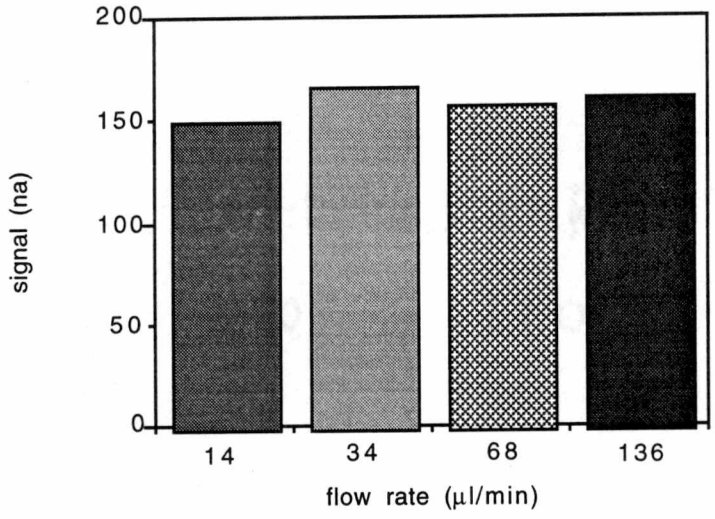

Figure 3.5. Effect of flow rate of 0.10 mg/ml TRITC-IgG on signal from immunobeads. Volume of TRITC-IgG for each sample was 50 µl. Rinse volume for each was 250 µl.

The calibration curves for aspirated samples of TRITC-IgG in PBS are shown in Figure 3.6. The values shown are averages for five trials at each concentration. CVs for these averages were in the range of 2.6-5.4 %. The curve for the 15 μl samples gave a correlation coefficient of 0.996 using linear regression analysis. The correlation coefficient for the 25 μl samples was 0.989. The "unknown" sample gave a signal of 64 na for a 15 μl sample, corresponding to a concentration of 0.028 mg/ml. For a 25 μl sample the signal was 72 na, corresponding to a concentration of 0.032 mg/ml. The concentration of the sample, as measured by UV absorbance at 280 nm, was 0.035 mg/ml. The curve for the lower sample volume had a smaller slope, indicating decreased sensitivity for the smaller volume. With the smaller sample volume, the maximum signal was also smaller, decreasing the signal to noise ratio for the method. For the measurements with this sensor the noise was between 1 and 2 na over an average background signal of 45 na.

The calibration curve for the more complex sample matrix is shown in Figure 3.7. A linear regression for this data gave a correlation coefficient of 0.978. An unknown sample in this matrix gave a signal of 112 na, indicating a concentration of 0.054 mg/ml of TRITC-IgG. The concentration of the sample was also measured using UV-VIS absorbance at 515 nm. This wavelength was chosen because of the other species in the sample that absorbed at 280 nm.

a)

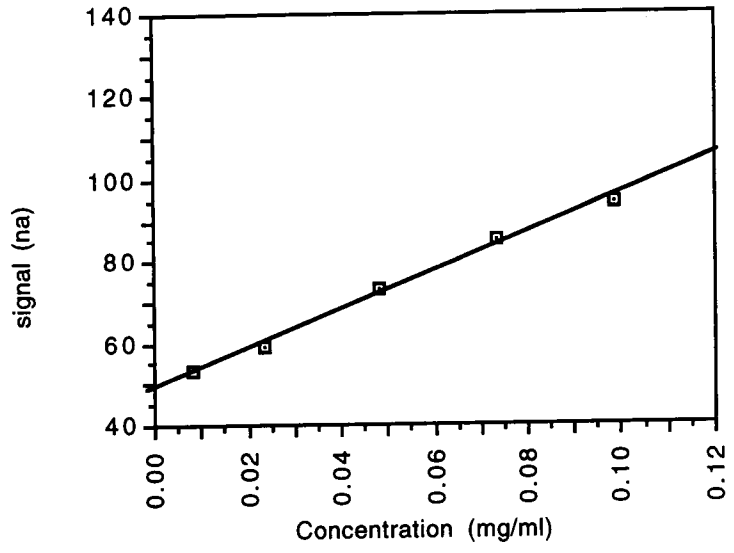

b)

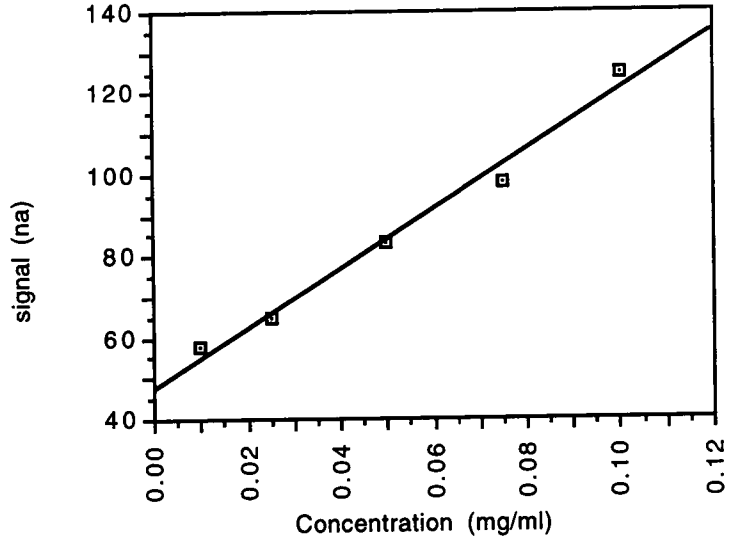

Figure 3.6. Calibration curve for TRITC-IgG in phosphate buffered saline. a) 15 µl sample size b) 25 µl sample size.

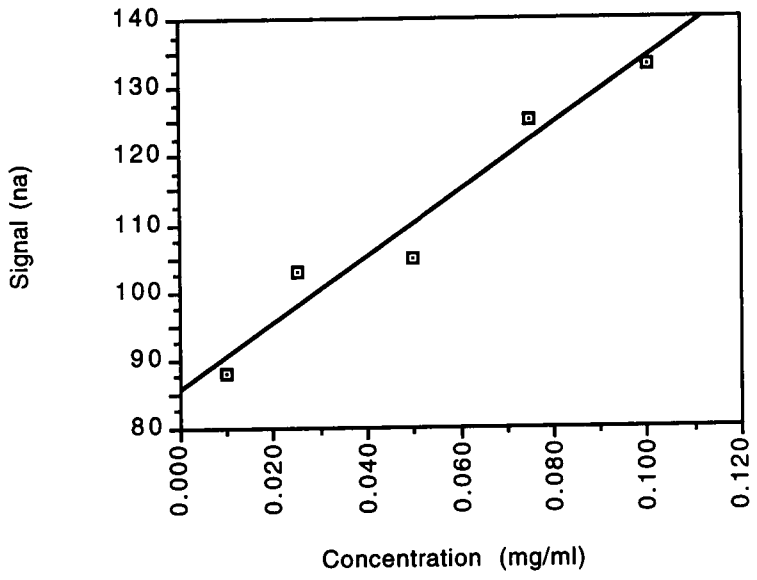

Figure 3.7. Calibration curve for 25 µl sample of TRITC-IgG in complex matrix.

Using this method the sample concentration was 0.062 mg/ml. The calibration curve has a smaller slope than either of the plots in PBS alone, indicating less sensitivity. This could be caused by non-specific binding of proteins other than the analyte to the antibody, perhaps covering analyte binding sites.

The direct assay of IgG helped to establish two parameters that would be helpful in the implementation of the sandwich assay. These were the effect of sample delivery flow rate on signal and optimum sample volume. The direct assay also indicated that there was sufficient sensitivity to distinguish between differing concentrations of analyte in the samples. The more complex matrix posed something of a problem in terms of sensitivity, but rather than pursue this problem further with the direct assay it was decided to proceed onward to the sandwich assay in hopes of improved sensitivity due to the inherent differences in the two assays.

Sandwich Assay

Experimental

The apparatus described above was modified slightly for the sandwich assay. Because a second antibody is needed in a sandwich assay it was necessary to add an additional 520 μm lead to the "T" assembly, turning it into an "X". The additional lead was used to

deliver the second antibody directly behind the sample, allowing it to follow the same path through the bead slurry.

The preliminary experiments for the sandwich assay were similar to those described for the direct assay. For the sandwich assay it was necessary to optimize the concentration and flow rate of the labeled second antibody (TRITC-Ab2). This was accomplished using batch immunobeads that contained Ab1 and IgG (prepared by incubating immunobeads in 0.10 mg/ml IgG). The TRITC-Ab2 concentration was held constant at 0.20 mg/ml, a large excess, and delivered at several different flow rates. Once an optimum flow rate was determined the TRITC-Ab2 concentration was varied at constant flow rate.

Once the flow rate and concentration for the TRITC-Ab2 were chosen a sandwich assay for IgG was performed as follows. 25 µl of sample was aspirated into the sample lead. 50 µl of immunobeads was then placed in the sensing chamber as with the direct assay. Sample was then returned to the sensing chamber, followed by the TRITC-Ab2. When the signal from the sensor began to increase rapidly, indicating that the leads from the X were filled with TRITC-Ab2, the rinse was turned on and the TRITC-Ab2 off. This allowed the rinse solution to follow the same path as the sample and TRITC-Ab2 through the immunobeads, pushing any TRITC-Ab2 left in the lead into the sensor ahead of it. This process was repeated for several different concentrations of IgG.

Results and Discussion

Figure 3.8 illustrates the effect of flow rate of TRITC-Ab2 on the signal from batch immunobeads that had been incubated with 0.10 mg/ml IgG. As was observed with the delivery of IgG in the direct assay, variation in flow rate caused very little change in the signal after rinsing. What did vary with flow rate in a somewhat surprising manner was the volume of rinse solution required to reach a stable signal. The total rinse volume ranged from approximately 170 µl (12 min) for the 14 µl/min flow rate to 204 µl (6 min) at 34 µl/min, 272 µl (4 min) at 68 µl/min, and 680 µl (5 min) for the 136 µl/min flow rate. One would expect that a faster flow rate would decrease the time to a stable signal since a larger volume of rinse would be delivered in less time. This was true in general. However, the shorter times and least volumes occurred at 34 and 68 µl/min. This affect was attributed to an increase in the turbulence of the flow with increasing flow rate. These small differences in rinse volume with flow rate might be significant, depending upon the application. If the sensor is to be used *in situ*, total rinse volume might become important relative to the total volume of the environment being sampled. For the remaining experiments in this report, the flow rate for all solutions was held constant at 68 µl/min, which appeared to be the best combination of short rinse time and fairly low volume.

The results of the experiment to determine optimum concentration of TRITC-Ab2 are shown in Figure 3.9. For batch beads

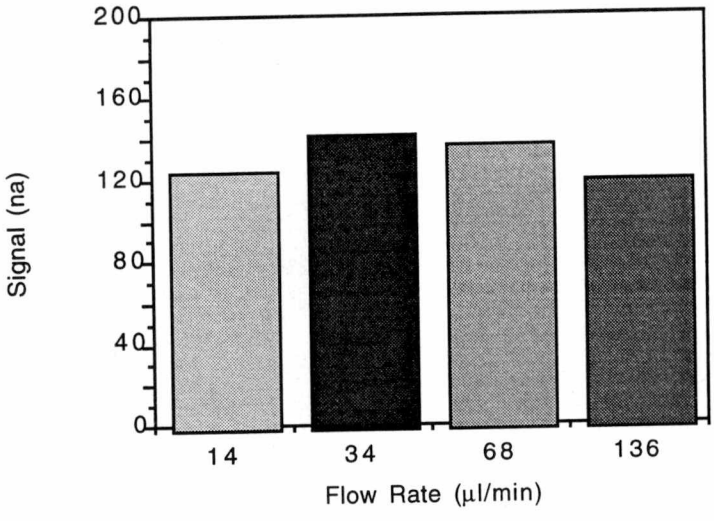

Figure 3.8. Effect of flow rate of TRITC labeled Anti-IgG on signal from batch immunobeads containing 0.10 mg/ml IgG.

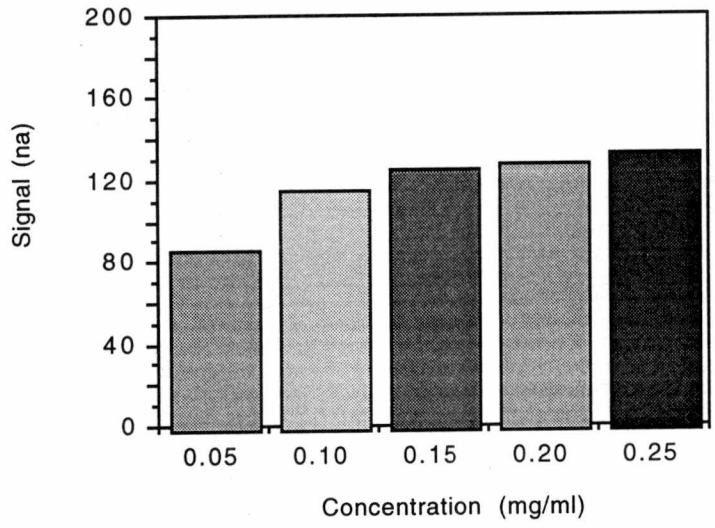

Figure 3.9. Effect on concentration of TRITC labeled anti-IgG on signal from batch immunobeads containing 0.10 mg/ml IgG.

exposed to 0.10 mg/ml IgG, the best concentration of TRITC-Ab2 seemed to be 0.15 mg/ml. Higher concentrations gave slight increases in signal, but it was unclear whether this was an increase in bound antibody or a rinsing problem. In addition, the size of the increase was not great enough to justify the added expense of the greater antibody concentration.

Table 3.8 summarizes the data from the complete sandwich assay of 0.10 mg/ml IgG. Reproducibility for this procedure was excellent, and the sensor flushed well between runs. As expected, the signal did not increase significantly until the addition of the TRITC-Ab2. Unlike the direct assay, where an increase in signal was observed when the sample was aspirated, there was no indicater of aspiration. The reproducibility of the final signal following rinse of the TRITC-Ab2 seemed to indicate that aspiration of sample had indeed occurred and that a sandwich assay, in which both antibodies to IgG were bound to the IgG, had been accomplished.

The results of a single experiment varying the concentration of IgG are shown in Figure 3.10. There was no apparent change in signal with concentration of IgG. These results are representative of those obtained when the experiment was repeated with 8 different batches of immunobeads, prepared at different times from two different preparations of diol silica. Two different lot numbers of anti-IgG were used. The lot number for the TRITC-antibody was the same, although the antibody was received in several shipments. Two different sensors were used after catastrophic failure of a sensor.

Table 3.8 Signal and Reproducibility data for isolated steps in sandwich assay using acrylic sensor with Teflon frit.

Measurement	Background signal (na)	Sample aspiration (na)[a]	Delivery of immunobeads (na)[b]	Delivery of sample (na)[c]	Delivery of TRITC-Ab2 max signal (na)[d]	Rinse (na)[e]	Flush (na)[f]
1	55	56	59	54	936	136	56
2	57	55	61	56	972	142	55
3	54	55	58	58	954	133	56
4	55	56	57	53	998	148	57
5	58	57	62	57	982	139	55
average	56	56	59	56	968	140	56
CV	2.9 %	1.5	3.5	3.7	2.5	4.1	1.5

Notes: See experimental section for more detail

a. 25 µl of 0.10 mg/ml IgG

b. 50 µl of immunobeads, bead density 10 mg/ml

c. Sample delivery rate 68 µl/min, delivery time 3 min (~200 µl)

d. 0.15 mg/ml TRITC-Ab2 delivered with flow rate of 68 µl/min, maximum signal occurred when sensor tip was filled with TRITC-Ab2

e. PBS rinse solution followed TRITC-Ab2, delivery started when signal from TRITC-Ab2 peaked, flow rate= 68 µl/min, total rinse time 6 min.

f. Sensor flushed with PBS solution until constant signal was obtained

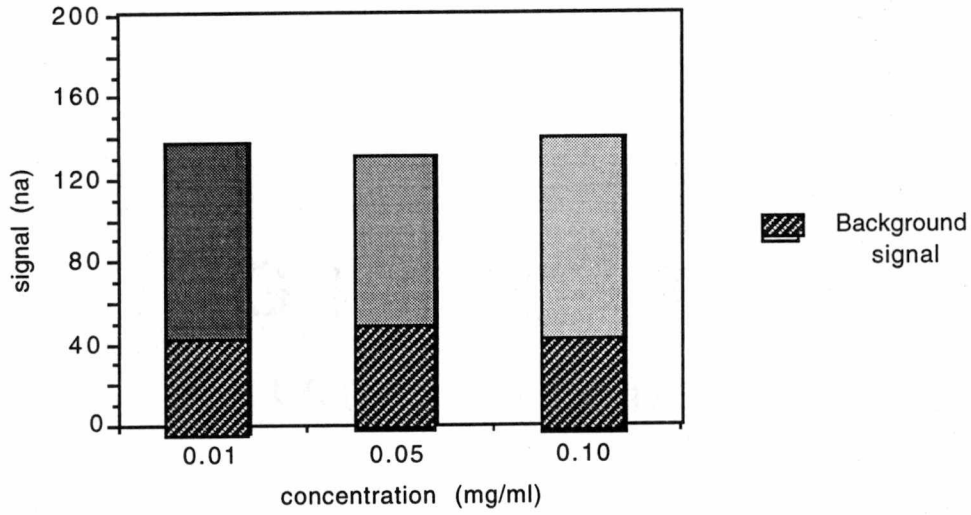

Figure 3.10. Sandwich assay for IgG. Variation of concentration of IgG. Concentration of TRITC labeled anti-IgG =0.15 mg/ml, Immunobead density=10 mg/ml, solution flow rate=68 μl/min.

Similar results were obtained for all; the only variation was the magnitude of signal and background between preparations of the immunobeads and between the two sensors. In all cases the signal for 0.10 mg/ml, 0.05 mg/ml and 0.01 mg/ml IgG were essentially the same.

In attempt to locate the source of the problem, some additional studies with the immunobeads and the sandwich system were done outside of the sensor. These experiments attempted to determine how much, if any, of each protein was binding to the immunobeads. It was suspected that the problem was with the second antibody, since variation in signal was seen for different concentrations of IgG in a direct assay. To verify that IgG was actually being bound to the immunobeads, the absorbance of 1 ml of IgG solution before a 5 minute incubation with 10 mg of immunobeads was compared to the absorbance afterwards. The amount bound was calculated from this difference. These beads were then incubated in 1 ml of TRITC-Ab2 solution for 5 minutes and the decrease in absorbance of this solution was used to calculate the amount of second antibody bound to the beads. The results of these experiments are shown in Table 3.9.

These results indicate that the problem was in the binding of the TRITC-Ab2. In theory the maximum binding capacity of the immunobeads should be equal to the amount of anti-IgG on the beads. Thus 10 mg of immunobeads with an antibody concentration of 4.6 mg/g should be able to bind a maximum of 0.046 mg of IgG. This is an

Table 3.9. Binding of proteins to immunobeads prepared from 80 Å pore size, 10 μm diameter Spherisorb™ silica.

Immunobead antibody concentration (mg Ab/g silica)[a]	Concentration of IgG solution (mg/ml)	Binding of IgG (mg IgG/g silica)[b]	Concentration of TRITC-Ab2 (mg/ml)	Binding of TRITC-Ab2 (mg Ab/g silica)[c]
4.6	0.025	2.4	0.05	1.4
			0.15	1.8
	0.050	3.2	0.05	1.5
			0.15	1.9
	0.10	3.9	0.05	1.5
			0.15	2.1
8.2	0.025	5.6	0.05	1.9
			0.15	2.4
	0.050	6.4	0.05	2.1
			0.15	2.4
	0.10	7.2	0.05	2.2
			0.15	2.3

Notes:

a. Determined by change in absorbance at 280 nm of anti-IgG solution during incubation with CDI activated diol-silica

b. Determined by change in absorbance at 280 nm of 1 ml of IgG solution following 5 min incubation with 10 mg of immunobeads.

c. Determined by change in absorbance at 280 nm of 1 ml of TRITC-labelled anti-IgG following 5 min incubation with beads from b.

amount much greater than the approximately 2 x 10^{-6}mg in the 0.01 mg/ml sample. One would also expect a similar ratio of IgG to the TRITC-labeled anti-IgG. The beads showed binding consistent with theory for the binding of IgG, but not of the second antibody. In these experiments the amount of TRITC-Ab2 bound seemed to depend more upon the initial antibody concentration than on the concentration of IgG, or of TRITC-Ab2.

The reasons for this are still unclear. One possibility is that there are steric problems with this particular sandwich assay on the silica spheres. In an attempt to increase the distance between antibody molecules and lower the binding of IgG while increasing binding of Ab2, 500 Å pore size silica, discarded earlier as having too small a binding capacity, was tested with the sandwich assay. The results of this experiment, identical in design to that described for 80 Å pore size silica, are shown in Table 3.10. There was no increase in the ratio of TRITC-Ab2 to IgG.

Another theory is that the use of polyclonal antibodies for both antibodies may be at the root of the problem. Polyclonal antibody solutions contain antibodies to a variety of epitopes on the same analyte molecule. This could mean that a single analyte might be able to bind to more than one antibody molecule in the solution. This is a requirement for sandwich assays; the two antibodies used must be specific to different portions of the analyte molecule. A monoclonal antibody solution contains antibodies that are all specific to the same epitope on the analyte molecule. In a solid

Table 3.10. Binding of proteins to immunobeads prepared from 500 Å pore size, 10 μm diameter Nucleosil™ silica.

Immunobead antibody concentration (mg Ab/g silica)[a]	Concentration of IgG solution (mg/ml)	Binding of IgG (mg IgG/g silica)[b]	Concentration of TRITC-Ab2 (mg/ml)	Binding of TRITC-Ab2 (mg Ab/g silica)[c]
3.5	0.025	2.1	0.05	1.4
			0.15	1.6
	0.050	2.7	0.05	1.3
			0.15	1.7
	0.10	3.4	0.05	1.5
			0.15	1.6

Notes:

a. Determined by change in absorbance at 280 nm of anti-IgG solution during incubation with CDI activated diol-silica

b. Determined by change in absorbance at 280 nm of 1 ml of IgG solution following 5 min. incubation with 10 mg of immunobeads.

c. Determined by change in absorbance at 280 nm of 1 ml of TRITC-labelled anti-IgG following 5 min incubation with beads from b.

phase sandwich assay the use of two monoclonal antibodies for different epitopes on the analyte insures that the sandwich assay will work. The use of a single monoclonal antibody, immobilized on the solid substrate, and polyclonal antibodies for the second antibody is the more common procedure. This research used polyclonal antibodies for immobilization on the immunobeads and polyclonal antibodies, labeled with TRITC, for the second antibody solution. The gamble was that there would be enough antibodies to a variety of epitopes on the IgG to allow two antibodies to bind to each IgG molecule. Using a large excess of the second antibody might increase the chances of antibodies being available to bind to the IgG; however, it might also increase the risk of nonspecific interactions and cause more difficulty rinsing out unbound reagents. The data from the binding experiments could indicate that there are not enough remaining sites on the IgG to bind with the TRITC-Ab, regardless of concentration.

A discussion with the technical support personnel at Sigma suggested another potential difficulty with this particular system. They are uncertain as to where the TRITC molecule binds to the antibody. They do know that there is an average of four TRITC molecules on each protein molecule. The TRITC could be covering some of the antibody's active sites. It was also suggested that non-specific binding of the IgG to the silica may be occurring to a significant extent, and that free TRITC label could be binding to the IgG causing an error in the signal from the TRITC-Ab2. TRITC is said

to be "very sticky" and it is difficult to remove all unbound fluorophore from the antibody solution. Monitoring the absorbance of the TRITC-Ab2 solution at 280 nm (where presumably the absorbance of the antibody was much greater than absorbance of the TRITC) was an attempt to guard against this error in the binding study, but there was no way to prevent it in the sensor. As for nonspecific binding, a quick binding experiment similar to those described above, but with no IgG solution, indicated that immunobeads containing 4.6 mg Ab1/g silica and no IgG could still bind approximately 0.5 mg Ab2/g silica. This indicated that non-specific binding was actually accounting for nearly one-half of the TRITC-Ab2 bound to the immunobeads.

The goal of the research in this chapter was to design a regenerable fiber optic sensor capable of use for a sandwich immunoassay of IgG. This goal was accomplished in part. The sensor seems to function well in the manner for which it was designed. The acrylic resin molding technique was more durable and allowed use of frit materials that were more amenable to protein analysis. The antibody immobilization studies gave some valuable insights into the limitations of solid phase antibodies, or at least those prepared using the techniques discussed herein. The sensor worked well for the direct assay of IgG. Unfortunately, there is not much use for a direct assay of proteins, since their native fluorescence is so weak.

The sandwich assay studies were an exercise in patience and detective work, with no clear answer obtained. With a more

appropriate antibody system the sensor might have been used sucessfully for a sandwich assay. Solid phase sandwich assays introduce many more variables into the design process than was initially perceived. Because of the bulk of the antibodies and analyte there is the potential for steric problems not encountered in direct assays. The choice of the antibodies is much more important in a sandwich assay than in a direct or competitive binding assay. The use of monoclonal antibodies might be required for a successful solid-phase sandwich immunoassay.

This brings us back to the immobilization procedure. As it now stands, there is a high risk that expensive antibody might be wasted if the immunobead immobilization procedure is not successful. During the course of this research there were at least as many, if not more, preparations of immunobeads that had to be discarded due to lack of binding of anti-IgG to the silica or loss of antibody activity as were used for the sensor experiments. It is also still unclear whether the use of monoclonal antibodies would even bring about improvement since the absence or presence of steric effects could not be demonstrated.

CHAPTER 4

CONCLUSIONS AND FUTURE STUDIES

The research reported in the previous chapters covers several approaches to the design of a fiber optic biosensor for large protein molecules such as antibodies. The goal was a sensor capable of continuous or repetitive measurements. The underlying assumption was that a sucessful sensor would also generate data that could be used to quantitate the protein concentration.

The analysis of proteins offers several problems that are less common with smaller molecules. The one of most interest to a spectroscopist is that protein absorbance and fluorescence are weak at best and frequently nonexistent, depending upon the presence of sufficient tyrosine, tryptophan, or phenyalanine amino acid residues to produce a measurable signal. Another important, but too frequently disregarded, characteristic is that proteins are often unstable when not in their native environment. This environment varies even within the organism producing the protein; a different environment is found in intracellular and extracellular fluid throughout the organism. If the protein's special requirements are not met outside its native environment it may denature and lose its distinguishing characteristics (61). Factors that were controlled as much as possible in this research were buffer pH, concentration, purity, and storage temperature. Recent information indicates that

the ionic strength of the buffer and the particular type of buffer are also very important for some proteins (61). Fortunately, phosphate buffered saline is very compatable with most antibodies and immunoglobulins are particularly hardy proteins.

The use of immunoassay to quickly identify and quantitate proteins is a well established technique. The ELISA and Western Blot methods are commonly used to test for hCG --an indicator of pregnancy, HIV antibodies, hepatitis B antibodies, and many other diagnostics (94). Some of these tests are used to measure the concentration of proteins, but more often they are used for a simple yes/no result--a particular antibody is present or not.

This raises the question of whether or not a method capable of rapid repeatable analysis of antibody concentration is necessary. Most clincal applications of antibody assays are concerned with the mere presence or absence of a given antibody. Antibody concentrations are not subject to rapid changes with disease progress. In most instances the concern is whether the subject was exposed to a particular analyte and developed antibodies to it. However, when an assay is performed, a standardization curve does indicate whether the observed binding is specific or nonspecific binding, thus validating the observation.

Concentration changes in proteins are of much greater interest to endocrinology researchers. The mechanism of action of many of the endocrine hormones is not completely understood. Some of the pituitary hormones are released in pulses rather than continuously

as was once believed. An inability to continuously monitor the hormone output and incorrect sampling intervals contributed to the delay in discovery of this characteristic. There may be other hormones that have pulsatile secretion (95). So, there is still a need for continous or rapidly repetitive analysis of proteins, just not the antibodies represented by the IgG molecule studied in this research.

As for the analysis of IgG by sandwich assay, the conclusion is that it may never work as designed. To understand this assertion, one must consider the immunological and spatial relationships involved. When antisera to IgG are developed and affinity purified, the antibodies are most likely to be specific to the constant region of the IgG molecule (see Figure 1.5), since the variable region will differ from molecule to molecule depending upon the analyte specificity of the IgG (since IgG is itself an antibody). Figure 4.1 is a model of what happens when this particular antibody-analyte system is used in a sandwich assay. When the antibodies to the IgG are immobilized and bind to the IgG, most can bind the constant region of two different IgG molecules. The second antibody to IgG in a sandwich assay will also try to bind to the constant portion of the IgG, but with very limited success. There is not room for it to access the desired binding sites. This explains why a direct assay for IgG works well, but a sandwich assay will not work. These steric limitations might be overcome by switching to monoclonal antibodies developed to the separate portions of the IgG molecule, particularly those specific to the F_{ab} portion.

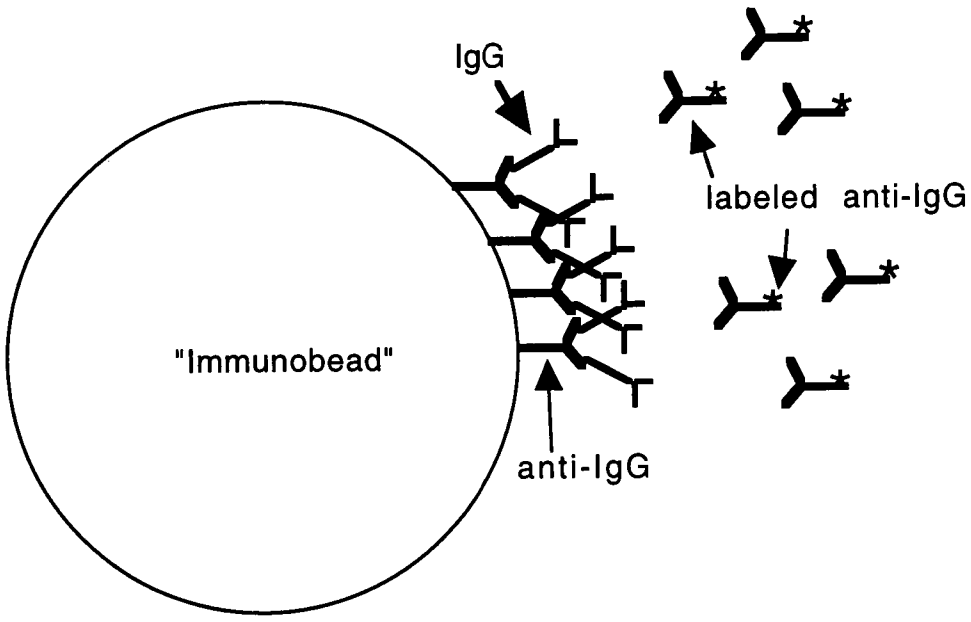

Figure 4.1. Sandwich assay for IgG on immunobead. Anti-IgG and labeled anti-IgG both need to bind to the constant region of the IgG molecule.

Given the need for analysis of endocrine hormones and the lack of need for a rapid analysis of most antibodies, perhaps the best approach for future research would be to choose a new antibody-analyte system, perhaps for a large hormone molecule that has two subunits such as the reproductive hormones follicle stimulating hormone (FSH) and leutinizing hormone (LH). Monoclonal antibodies to the different subunits should be available; however one should be aware that these two hormones have a common subunit, so the choice of immobilized antibody would be critical. Even with antibodies developed to widely separated epitopes such as those on FSH or LH, there are likely to be steric problems for a sandwich assay using two antibodies to the same analyte. These molecules have molecular weight of around 25,000 daltons, compared to IgG with a molecular weight of 160,000.

Some "sandwich" assays do not actually use two antibodies to the same analyte. Instead the second antibody is an antibody against the first antibody which is already bound to analyte. If a mixing chamber were added so that the fluorescently labeled antibody were mixed with the analyte from sample before contact with immunobeads with antibody specific to the labeled antibody, this type of sandwich assay might work in the sensor described in Chapter 3. It might however be impossible to distinguish the antibody bound to the analyte from unbound antibody. The body has a

natural method of distinguishing bound from unbound antibody in a product called complement; perhaps this could be used to separate bound from unbound analyte. Either of these modifications would make an already complex assay protocol even more complicated. This would almost certainly make the requirement of a rapidly repeatable sensor out of reach.

Before any further research is conducted into sandwich assays, the difficulties in immunobead preparation need to be overcome. Perhaps use of a commercially available product is a future option. Affinity chromatography media with appropriate antibodies already immobilized would be highly desirable. It may be that particles with appropriate antibodies already attached will be commercially available soon, or that the process could be contracted out to a company that prepares affinity chromatography media. One major difference between affinity chromatography media and media for sandwich assay is the purpose of the immobilized antibody. In affinity chromatography there is less concern about which portion of the analyte binds to the antibody, since the goal is to separate analyte from whole sera or some other matrix and then to collect the analyte outside of the column. There is no need for a second antibody reaction while the analyte is immobilized. This allows the use of polyclonal antibodies or monoclonals to a region on the constant region of the antibody.

Most affinity chromatography media are not spherical silica. It is likely that spherical silica is no longer a hard and fast

requirement given the improved sensor design. It was originally necessary because the cylindrical frit sensor described in Chapter 2 would not flush out well with any other media. Also tested at that time were polycarbonate microspheres with carboxylate groups available for derivatization (Polysciences Inc, Warrington PA). The spheres would not flush out of the sensor, so were not pursued further at that time. They might be more compatible with the acrylic sensor described in Chapter 3 and would give better binding of antibody with less loss of activity. The method for coupling antibody to these particles is also a carbodiimide linkage, but takes only about 3 hours for the entire process. Because the linkage is also a Schiff-base, there might still be difficulty with loss of antibody activity during coupling. Considering the steric problems encountered so far, loss of some antibody activity might not be all bad. The less active antibody present, the further apart the bound molecules are and the better the chance of the second antibody finding room to react. This phenomenon was noted with several of the immunobead samples in this research; more immobilized antibody was not always better. The smaller immunobead coverages bound a higher percentage of IgG than those with more immobilized antibody. Reducing the total antibody coverage on the silica might actually improve signal rather than causing a decrease as was expected.

The design of a sandwich immunoassay requires many more steps than are required for a direct assay. The number of factors to

be controlled expands almost exponentially with the need for binding of a second antibody. Conditions that worked well for a direct assay of the same analytes became hindrances to the sucess of a sandwich assay. Factors that were minor annoyances in the direct assay could be expensive deterents to a sandwich assay.

The regenerable biosensor described in Chapter 3 works very well for direct assays as has been shown by this researcher and others. Perhaps it is more important to emphasis the sucess of the sensor for this type of assay rather than concentrate on the failure of the sandwich assay. There are a number of non-clinical uses for a sensor capable of direct assays and many more fluorescent analytes available in non-clinical settings. Improvements in detection optics might also make direct fluorescence analysis of biomolecules more accessible in the future.

REFERENCES

REFERENCES

1. O. S. Wolfbeis, in *Fiber Optic Chemical Sensors and Biosensors*, O. S. Wolfbeis, Eds. (CRC Press, Boca Raton, 1991), 1.

2. A. P. F. Turner, *Sensors and Actuators* **17**, 433 (1989).

3. M. A. Arnold, M. E. Meyerhoff, *CRC Crit. Rev. Anal. Chem.* **20**, 149 (1988).

4. O. Parriaux, in *Fiber Optic Sensors and Biosensors*, O. S. Wolfbeis, Eds. (CRC Press, Boca Raton, 1991), 111.

5. R. A. Lieberman, in *Fiber Optic Chemical Sensors and Biosensors*, O. S. Wolfbeis, Eds. (CRC Press, Boca Raton, FL, 1991), 193.

6. J. D. Andrade, R. A. Vanwagenen, D. E. Gregonis, K. Newby, J. N. Lin, *IEEE Trans. Elec. Dev.* **32**, 1175 (1985).

7. F. V. Bright, K. S. Litwiler, *Anal. Chem.* **61**, 1510-1513 (1989).

8. G. Boisde, F. Blanc, J.-J. Perez, *Talanta* **35**, 75 (1988).

9. J. F. Giuliani, P. P. Bey Jr., *Appl. Opt.* **27**, 1353-1357 (1988).

10. J. E. Freeman, A. G. Childers, A. W. Steele, G. M. Hieftje, *Anal. Chim. Acta* **177**, 121-128 (1985).

11. H. Tai, H. Tanaka, T. Yoshino, *Opt. Lett.* **12**, 437 (1987).

12. K. A. Saturday, *Anal. Chem.* **55**, 2459 (1983).

13. W. A. Chudyk, M. M. Carrabba, J. E. Kenny, *Anal. Chem.* **57**, 1237 (1985).

14. C. Gomy, M. Jouan, N. Q. Dao, *Anal. Chim. Acta* **215**, 211 (1988).

15. J. T. Coleman, J. F. Eastham, M. J. Sepaniak, *Anal. Chem.* **56**, 2246-2249 (1984).

16. B. J. Tromberg, J. F. Eastham, M. J. Sepaniak, *Appl. Spectrosc.* **38**, 38-42 (1984).

17. O. S. Wolfbeis, in *Fiber Optic Chemical Sensors and Biosensors*, O. S. Wolfbeis, Eds. (CRC Press, Boca Raton, Fl, 1991), 61-110.

18. R. D. Petrea, M. J. Sepaniak, T. Vo-Dinh, *Talanta* **35**, 139-144 (1988).

19. T. Vo-Dinh, *et al.*, *Appl. Spectrosc.* **41**, 735-738 (1987).

20. M.-R. S. Fuh, L. W. Burgess, G. D. Christian, *Anal. Chem.* **60**, 433-435 (1988).

21. K. R. Rogers, J. J. Valdes, M. E. Eldefrawi, *Anal. Biochem.* **182**, 353-359 (1989).

22. S. Klainer, M. Harris, in *Optical Fibers in Medicine III* (SPIE, Los Angeles, 1988), 138.

23. R. R. Smardzewski, *Talanta* **35**, 95 (1988).

24. D. Meadows, J. S. Schultz, *Talanta* **35**, 145-150 (1988).

25. T. E. Edmonds, N. J. Flatters, C. F. Jones, J. N. Miller, *Talanta* **35**, 103 (1988).

26. M. S. Abdel-Latif, A. A. Suleiman, G. G. Guilbault, *Anal. Lett.* **21**, 943-951 (1988).

27. J. Wangsa, M. A. Arnold, *Anal. Chem.* **60**, 1080-1082 (1988).

28. L. J. Blum, S. M. Gautier, P. R. Coulet, *Anal. Lett.* **21**, 717-726 (1988).

29. S. Luo, D. R. Walt, *Anal. Chem.* **61**, 174-177 (1989).

30. S. Luo, D. R. Walt, *Anal. Chem.* **61**, 1069-1072 (1989).

31. F. L. Dickert, E. H. Lehmann, S. K. Schreiner, H. Kimmel, G. R. Mages, *Anal. Chem.* **60**, 1377-1380 (1988).

32. O. S. Wolfbeis, A. Sharma, *Anal. Chim. Acta* **208**, 53-58 (1988).

33. U. J. Krull, R. S. Brown, A. Safarzadeh-Amiri, in *Optical Fibers in Medicine III*, A. Katzir, Ed. (SPIE, Los Angeles, 1988), 49.

34. D. R. Walt, S. Luo, C. Munkholm, in *Optical Fibers in Medicine*, A. Katzir, Ed. (SPIE, Los Angeles, 1988), 60.

35. M. Arnold, in *Optical Fibers in Medicine III*, A. Katzir, Ed. (SPIE, Los Angeles, 1988), 128.

36. N. Opitz, D. W. Lubbers, *Talanta* **35**, 123-127 (1988).

37. T. Jones, M. D. Porter, *Anal. Chem.* **60**, 404-406 (1988).

38. M. A. Arnold, T. J. Ostler, *Anal. Chem.* **58**, 1137-1140 (1986).

39. T. D. Rhines, M. A. Arnold, *Anal. Chim. Acta* **231**, 231-235 (1990).

40. B. J. Tromberg, M. J. Sepaniak, J. P. Alarie, T. Vo-Dinh, R. M. Santella, *Anal. Chem.* **60**, 1901-1908 (1988).

41. J. S. Schultz, S. Mansouri, I. J. Goldstein, *Diabetes Care* **5**, 245 (1982).

42. M. K. Carroll, F. V. Bright, G. M. Hieftje, *Anal. Chem.* **61**, 1768-1772 (1989).

43. B. S. Walters, T. J. Nielson, M. A. Arnold, *Talanta* **35**, 151 (1988).

44. W. Trettnak, O. S. Wolfbeis, *Fresnius Z. Anal. Chem.* **334**, 427 (1989).

45. R. Narayanaswamy, D. A. Russell, F. Sevilla, *Talanta* **35**, 83-88 (1988).

46. J. I. Peterson, S. R. Goldstein, R. V. Fitzgerald, *Anal. Chem.* **52**, 864-869 (1980).

47. D. M. Jordan, D. R. Walt, *Anal. Chem.* **59**, 437-439 (1987).

48. L. A. Saari, W. R. Seitz, *Anal. Chem.* **54**, 821-823 (1982).

49. G. Serra, A. Schirone, R. Boniforti, *Anal. Chim. Acta* **232**, 337-344 (1990).

50. Z. Zhujun, W. R. Seitz, *Anal. Chim. Acta* **160**, 47 (1984).

51. D. C. Ashworth, H. P. Huang, R. Narayanaswamy, *Anal. Chim. Acta* **213**, 251-257 (1988).

52. F. V. Bright, G. E. Poirier, G. M. Hieftje, *Talanta* **35**, 113-118 (1988).

53. Y. Kawabata, R. Tahara, T. Imasaka, N. Ishibashi, *Anal. Chim. Acta* **212**, 267-271 (1988).

54. L. A. Saari, W. R. Seitz, *Anal. Chem.* **56**, 810-813 (1984).

55. K. Suzuki, *et al.*, *Anal. Chem.* **61**, 382-384 (1989).

56. Z. Zhujun, W. R. Seitz, *Anal. Chim. Acta* **171**, 251-258 (1985).

57. E. Urbano, H. Offenbacher, O. S. Wolfbeis, *Anal. Chem.* **56**, 427-429 (1984).

58. W. A. Wyatt, F. V. Bright, G. M. Hieftje, *Anal. Chem.* **59**, 2272-2276 (1987).

59. E. Koller, O. Wolfbeis, in *Fiber Optic Chemical Sensors and Biosensors*, O. S. Wolfbeis, Eds. (CRC Press, Boca Raton, 1991), 303.

60. O. S. Wolfbeis, L. J. Weis, M. J. P. Leiner, W. E. Ziegler, *Anal. Chem.* **60**, 2028-2030 (1988).

61. D. M. Bollag, S. J. Edelstein, *Protein Methods* (Wiley-Liss, Inc, New York, 1991).

62. U. J. Krull, R. S. Brown, E. T. Vandenberg, in *Fiber Optic Chemical Sensors and Biosensors,* O. S. Wolfbeis, Eds. (CRC Press, Boca Raton, 1991), 315.

63. M. A. Arnold, *Anal. Chem.* **57**, 565-566 (1985).

64. O. S. Wolfbeis, *Anal. Chem.* **58**, 2874 (1986).

65. R. Sutherland, C. Dahne, J. F. Place, A. S. Ringrose, *Clin. Chem.* **30**, 1533(1984).

66. R. G. Eenink, H. E. De Brujin, R. P. H. Kooyman, J. Greve, *Anal. Chim. Acta* **238**, 317-321 (1990).

67. A. N. Sloper, J. K. Deacon, M. T. Flanagan, *Sens. Actuators* **B**, 1-6 (1990).

68. F. P. Anderson, W. G. Miller, *Clin. Chem.* **34**, 1417-1421 (1988).

69. W. G. Miller, F. P. Anderson, *Anal. Chim. Acta* **227**, 135 (1989).

70. T. A. Betts, *et al.*, *Anal. Chim. Acta* **246**, 55 (1991).

71. J. P. Alarie, J. R. Bowyer, M. J. Sepaniak, A. H. Hoyt, T. Vo-Dinh, *Anal. Chim. Acta* **236**, 237-244 (1990).

72. B. J. Tromberg, M. J. Sepaniak, T. Vo-Dinh, in *Optical Fibers in Medicine III*, A. Katzir, Eds. (SPIE, Los Angeles, 1988), 6.

73. T. Vo-Dinh, G. D. Griffin, K. R. Ambrose, *Appl. Spectrosc.* **40**, 696-700 (1986).

74. T. Vo-Dinh, *et al.*, in *The 11th International Symposium on PAHs*, Gaithersburg, MD, 1987),

75. T. Vo-Dinh, *et al.*, in *SPIE* A. Katzir, Eds. (ACS, Los Angeles, 1988), 18

76. T. Vo-Dinh, T. Nolan, Y. F. Cheng, M. J. Sepaniak, J. P. Alarie, *Appl. Spectrosc.* **44**, 128 (1990).

77. T. Vo-Dinh, J. P. Alarie, R. W. Johnson, M. J. Sepaniak, R. M. Santella, *Clin. Chem.* **37**, 532 (1991).

78. J. R. Bowyer, J. P. Alarie , M. J. Sepaniak , T. Vo-Dinh, R. Q. Thompson, *Analyst* **116**, 117-127 (1991).

79. N. Nakamura, T. Matsunaga, *Anal. Lett.* **24**, 1075 (1991).

80. D. Chan W., in *Immunoassay A Practical Guide,* D. Chan W., M. Perlstein T., Eds. (Academic Press, Inc, Orlando, FL, 1987),

81. W. P. Collins, *Alternative Immunoassays* (John Wiley & Sons, New York, 1985).

82. E. M. Chait, R. C. Ebersole, *Anal. Chem.* **53**, 682A-692A (1981).

83. G. Zubay, in *Biochemistry* (Wm. C. Brown, Dubuque, IA, 1993), 963.

84. C. Papadea, I. J. Check, *Crit. Rev. Clin. Lab. Sci.* **27**, 27 (1989).

85. I. Hemmila, *Clin. Chem.* **31**, 359-370 (1985).

86. K. Mosbach, in *Methods in Enzymology,* S. P. Colowick, N. O. Kaplan, Eds. (Academic Press, New York, 1976), 999.

87. B. J. Tromberg, M. J. Sepaniak, T. Vo-Dinh, G. D. Griffin, *Anal. Chem.* **59**, 1226-1230 (1987).

88. J. R. Bowyer, in *Construction, Evaluation, and Use of a Fluoroimmunochemical-Based Fiber Optic Microscale Regenerable Sensor* , University of Tennessee, PhD Disseration (1991).

89. J. A. Alarie, M. J. Sepaniak, T. Vo-Dinh, *Anal. Chim. Acta* **229**, 169-176 (1990).

90. K. Mosbach, in *Methods in enzymology,* K. Mosbach, Eds. (Academic Press, New York, 1976), 999.

91. J. R. Sportsman, G. S. Wilson, *Anal. Chem.* **52**, 2013 (1980).

92. S. C. Crowley, K. C. Chan, R. R. Walters, *J. Chromatography* **359**, 359 (1986).

93. Solomons, T.W. Graham, in *Organic Chemistry* (John Wiley and Sons, New York, 1980) 805

94. Ngo, T. T., in *Enzyme Mediated Immunoassay: An Overview* (Plenum Press, New York, 1985) 3-32

95. Berne, Robert M. , Levy, Matthew N., in *Physiology* (C. V. Mosby, St. Louis, 1983) 989-990

VITA

Melissa McManis Armstrong was born in Germany and raised in Virginia. She graduated from Liberty High School in Bedford, Virginia in 1980 and attended Davidson College in North Carolina, receiving a BS in Chemistry in 1984. In the fall of 1984, she entered graduate school in Chemistry at the University of Tennessee. While in graduate school she was active at Second Presbyterian Church in Knoxville, where she met her future husband, Jeffrey D. Armstrong. They were married in May 1991, and moved to Charlotte, North Carolina in August 1991.

Mrs. Armstrong has been employed by Gaston College in Dallas, North Carolina as an Instructor of Chemistry since August 1991. She is active in her church and community, serving as a Sunday School teacher and curriculum planner, and working with Habitat for Humanity of Charlotte, Crisis Assistance Ministries, and Loaves and Fishes. She is a member of the American Chemical Society and the North Carolina Education Association, and is Recording Secretary for PEO Chaper R in Charlotte NC.